energies

MDPI

Review

Application of Machine Learning in Fuel Cell Research

Danqi Su †, Jiayang Zheng †, Junjie Ma, Zizhe Dong, Zhangjie Chen and Yanzhou Qin *

State Key Laboratory of Engines, Tianjin University, Tianjin 300350, China
* Correspondence: qinyanzhou@tju.edu.cn
† These authors contributed equally to this work.

Abstract: A fuel cell is an energy conversion device that utilizes hydrogen energy through an electrochemical reaction. Despite their many advantages, such as high efficiency, zero emissions, and fast startup, fuel cells have not yet been fully commercialized due to deficiencies in service life, cost, and performance. Efficient evaluation methods for performance and service life are critical for the design and optimization of fuel cells. The purpose of this paper was to review the application of common machine learning algorithms in fuel cells. The significance and status of machine learning applications in fuel cells are briefly described. Common machine learning algorithms, such as artificial neural networks, support vector machines, and random forests are introduced, and their applications in fuel cell performance prediction and optimization are comprehensively elaborated. The review revealed that machine learning algorithms can be successfully used for performance prediction, service life prediction, and fault diagnosis in fuel cells, with good accuracy in solving nonlinear problems. Combined with optimization algorithms, machine learning models can further carry out the optimization of design and operating parameters to achieve multiple optimization goals with good accuracy and efficiency. It is expected that this review paper could help the reader comprehend the state of the art of machine learning applications in fuel fuels and shed light on further development directions in fuel cell research.

Keywords: fuel cells; machine learning; neural networks; support vector machines; random forests

check for updates

Citation: Su, D.; Zheng, J.; Ma, J.; Dong, Z.; Chen, Z.; Qin, Y. Application of Machine Learning in Fuel Cell Research. *Energies* **2023**, *16*, 4390. https://doi.org/10.3390/en16114390

Academic Editor: Nicu Bizon

Received: 31 January 2023
Revised: 10 May 2023
Accepted: 23 May 2023
Published: 29 May 2023

Copyright: © 2023 by the authors. Licensee MDPI, Basel, Switzerland. This article is an open access article distributed under the terms and conditions of the Creative Commons Attribution (CC BY) license (https://creativecommons.org/licenses/by/4.0/).

1. Introduction

The primary energy consumption on earth has been increasing since the industrial revolution, which has created serious social problems such as environmental pollution and global climate change [1]. Developing clean and renewable energy sources and conversion techniques is becoming a necessity for the survival of human beings. The rational utilization of hydrogen energy is conducive to solving the problems of energy shortages, environmental pollution, and global warming [2–4]. A fuel cell is an energy conversion device that utilizes hydrogen energy through an electrochemical reaction. Despite their many advantages, such as high efficiency and zero emissions, fuel cells have not yet been fully commercialized due to their deficiencies in service life, cost, and performance. Efficient evaluation methods for performance and service life are critical for the design and optimization of fuel cells.

Based on the electrolytes used, fuel cells are mainly divided into polymer electrolyte membrane (PEM) fuel cells (PEMFCs), solid oxide fuel cells (SOFCs), alkaline fuel cells (AFCs), phosphoric acid fuel cells (PAFCs), and molten carbonate fuel cells (MCFCs). PEMFCs are the most commercialized in vehicular applications and feature the advantages of a high electrical energy conversion efficiency, high power density, low operating temperature, and fast startup process. PEMFCs are mainly composed of a PEM, catalyst layer (CL), gas diffusion layer (GDL), and bipolar plate (BP). Single cells are assembled to form a fuel cell stack, as shown in Figure 1.

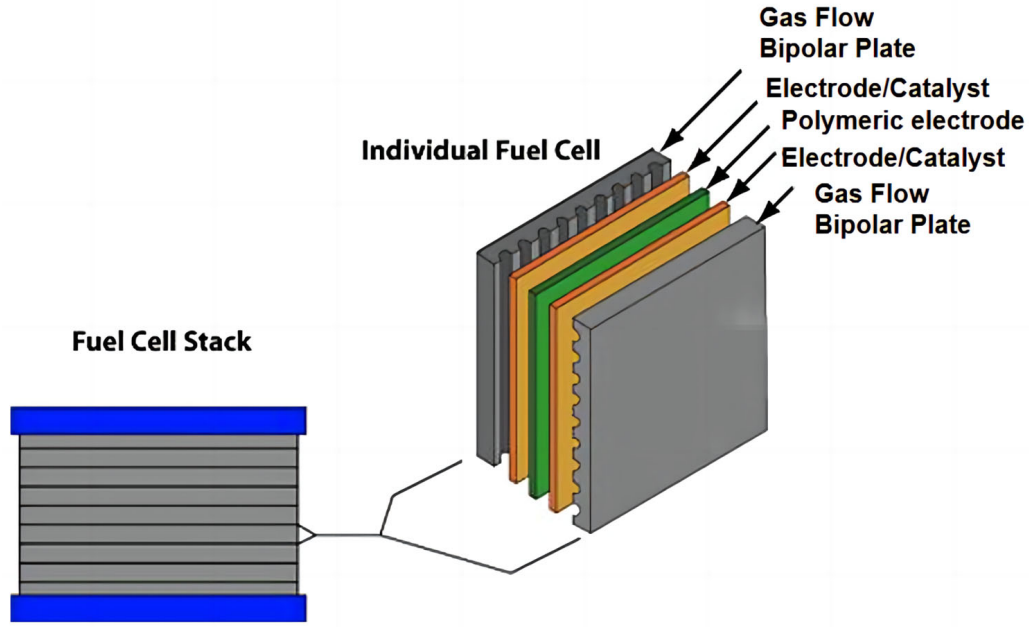


Figure 1. Schematic of single fuel cell and fuel cell stack.

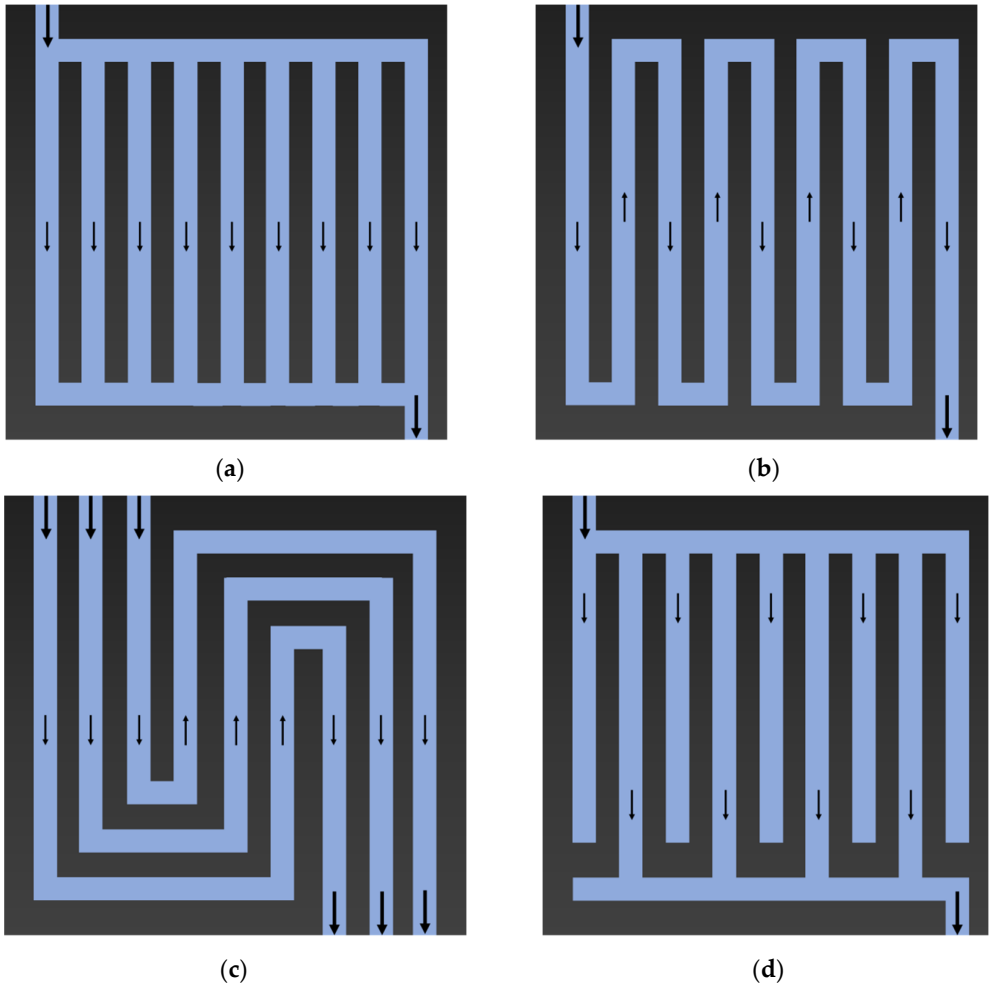


Figure 2. Common flow field patterns: (**a**) parallel flow field; (**b**) serpentine flow field; (**c**) parallel serpentine flow field; and (**d**) interdigital flow field.

The current research on fuel cells is extensive, including fuel cell material [5,6], flow channel [7], stack [8], system [9], and even fuel cell vehicle [10] design and optimization. Fuel cells' component designs are particularly important to their performance. For example, the flow field carved into the BP supplies oxygen and hydrogen to the porous electrode to maintain the normal operation of the fuel cell. Different flow field designs cause different reactant gas distributions and pressure drops. A poorly designed flow field results in uneven gas distribution, leading to uneven electrochemical reactions in the CL, which significantly decreases fuel cell performance, stability, and service life. The common flow field designs mainly include parallel flow fields, serpentine flow fields, parallel serpentine flow fields, and interdigitated flow fields, as shown in Figure 2. In addition to the traditional flow fields, many new flow fields have attracted the attention of researchers, such as lung bionic flow fields, leaf vein bionic flow fields, and intestinal system bionic flow fields [11,12], as illustrated in Figure 3. The flow field pattern, channel number, channel cross-section shape and area, channel/rib ratio, and surface wettability are all important design parameters.

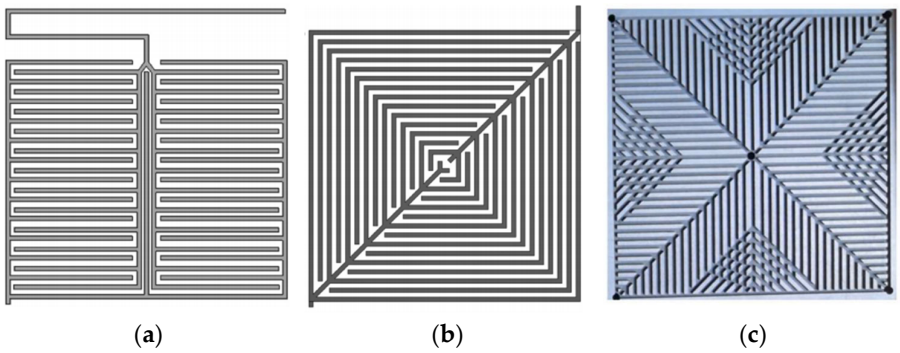


Figure 3. Bionic flow field patterns: (**a**) lung bionic flow field [11]; (**b**) leaf vein bionic flow field [11]; and (**c**) intestinal system bionic flow field [12].

In the optimization of membrane electrode assembly (MEA), the reasonable design of the porosity, thickness, and wettability of the CL and GDL can help improve the water management and output performance of fuel cells [13]. Regarding fuel cell system control technology, the control objects are focused on the concentration, pressure, temperature, and humidity, which involves many system components, such as air compressors, water pumps, cooling fans, and humidifiers. Various control techniques are used to maintain the stack working conditions, such as keeping the temperature and humidity close to the optimum level, to obtain the optimal fuel cell stack output performance [9].

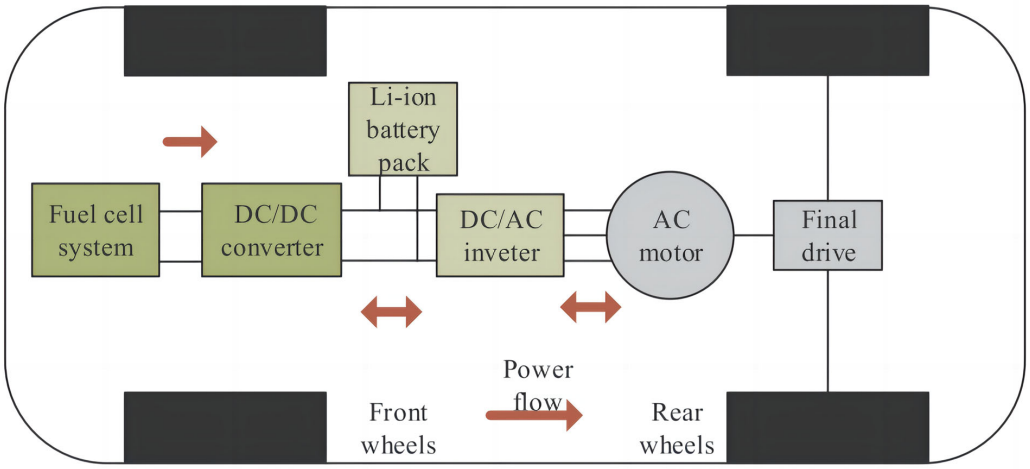


Figure 4. Structure of a fuel cell hybrid vehicle [14].

Fuel cell vehicles mainly adopt an electric–electric hybrid power system configuration consisting of a fuel cell and a power battery, the structure of which is shown in Figure 4. The fuel cell is connected to the DC bus through a unidirectional DC/DC converter, and the lithium battery is directly connected to the DC bus. They can both drive the motor through an inverter, which serves to convert the current between AC and DC. Coordinating the energy distribution between the fuel cell and power battery is the key to achieving a good level of power and economy for the vehicle, so energy management is one of the core technologies. The reasonable allocation of energy to the power source is a key technology to ensure the reliable operation of fuel cell vehicles [14].

Fuel cells are complex, with coupling problems numbering among the many design and operating parameters, and their efficient multi-objective optimization is difficult using traditional methods. Applying machine learning methods to train data-driven agent models has shown accuracy comparable to that of physical models and experimental tests, and data-driven agent models can complete most of the computations within one second, while physical CFD models and experimental tests may take hundreds of hours. This greatly improves the computational efficiency and can be widely used for the multi-variate optimization of complex fuel cell systems [15].

2. Status of Machine Learning Applications in Fuel Cells

Machine learning is a method that applies model training to obtain a certain data-fitting model based on existing data and uses this model to execute predictions with high nonlinear problem forecasting accuracy and computational efficiency. Machine learning models are widely used to predict fuel cell performance, ageing, and fault diagnosis. Kong et al. [16] proposed an artificial neural network (ANN) model for estimating the relationship between current and temperature in fuel cells. The model predicted voltages that matched the actual values fairly well, with a maximum relative voltage error of less than 8%. A support vector machine regression (SVR) model was proposed to predict the nonlinear dynamic characteristics of solid oxide fuel cells (SOFCs) by Huo et al. [17], and an improved particle swarm optimization (PSO) algorithm was then used to optimize the parameters in the model during training, which in turn improved the prediction accuracy. The PSO algorithm was found to be superior to the cross-validation method in the selection of SVR model parameters. In addition, Kheirandish et al. [18] used SVR to predict the performance of a nonlinear, multivariate predictive proton exchange membrane fuel cell (PEMFC) system for commercial electric bicycles. In the SVM prediction model, the coefficient of determination of the power–current curve was about 99%, while in the MLP model it was about 97%. Ding et al. [19] used machining learning approaches to solve the coupling problems associated with platinum-based catalysts in PEMFCs in order to minimize experimental costs in the face of numerous interacting parameters, and nine different machine learning algorithms were applied to obtain accurate prediction models and determine the optimal synthesis conditions. Chen et al. [20] first proposed a method for predicting voltage consistency by machine learning using CFD approaches to provide source data for the prediction model; then, they trained a gradient-boosted decision tree integrated model and finally carried out predictions using the developed model. Its accuracy was 0.901, higher than that of other methods. Raeesi et al. [21] used experimental data to train a deep neural network model, which was in turn used to predict fuel cell degradation in hydrogen passenger vehicles. Li et al. [22] used the SVR approach for fault diagnosis and fault type detection in PEMFC systems and validated the model by experiments on 40 fuel cell stacks; the accuracy of the prediction was 95.306. Zheng et al. [23] used SVR for the fault diagnosis of multivariate strongly coupled SOFC systems, and the results showed that the method had high accuracy, with an error detection rate of less than 7%. Chen et al. [24] proposed an optimization framework based on SVR and the gray wolf optimization algorithm to predict the remaining life of fuel cells, with an average absolute percentage error of less than 0.3%, effectively improving the accuracy of predicting the remaining life of degraded fuel cells.

The above analysis shows that machine learning models have been successfully used for performance prediction, aging prediction, and fault diagnosis in fuel cells, achieving good accuracy when solving nonlinear problems. Combined with optimization algorithms, machine learning models can further carry out the optimization of design and operating parameters to achieve multiple optimization goals with good accuracy and efficiency.

3. Common Machine Learning Models

3.1. Neural Network Model

Neural networks are a mathematical model for information processing similar to biological neural networks, belonging to a branch of machine learning that can process nonlinear functions based on the obtained input and output information and map the input and output well. They contain three parts: the input layer, hidden layer, and output layer, where the neurons in the hidden layer can receive information from the previous layer and output to the next layer. As a typical neural network, an artificial neural network (ANN) is a deep learning algorithm that, as presented in Figure 5, is a subset of machine learning [25]. As illustrated in Figure 6, based on the combination of neurons in the hidden layer, ANNs successfully achieve the fitting of the objective function and further deduce the mapping relationship between the input and output.

$$y_j = f\left(\sum_{i=1}^{n} x_i w_{ij} - \theta_j\right) \tag{1}$$

where x_i denotes the neuron input variables; y_j the neuron output variables; w_{ij} the weight between the jth neuron from which the input is taken and the ith neuron; θ_j the threshold value; and f the activation function, generally chosen to be nonlinear.

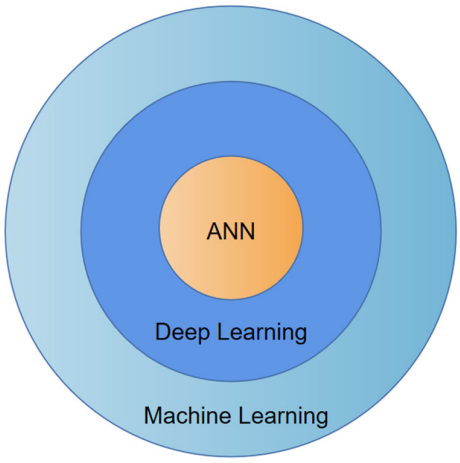


Figure 5. ANN as a subset of machining learning.

The three most popular network architectures are single-layer feedforward networks, multi-layer feedforward networks, and recurrent networks. In 1986, Rumelhart et al. [26] proposed an algorithm to optimize the network parameters of a neural network model layer by layer: the error back-propagation algorithm (BPA). A specific example of back-propagation is shown in Figure 7. In the network training process, the error cost function between the output value of the network model and the expected value is first calculated, and then the error cost function is back-propagated. In the back-propagation process, the stochastic gradient descent method is used to continuously update the gradient of each layer. The back-propagation process uses stochastic gradient descent to continuously update the weight coefficients and bias of each layer, so that the error cost function of the neural network reaches the minimum value and achieves adaptive learning.

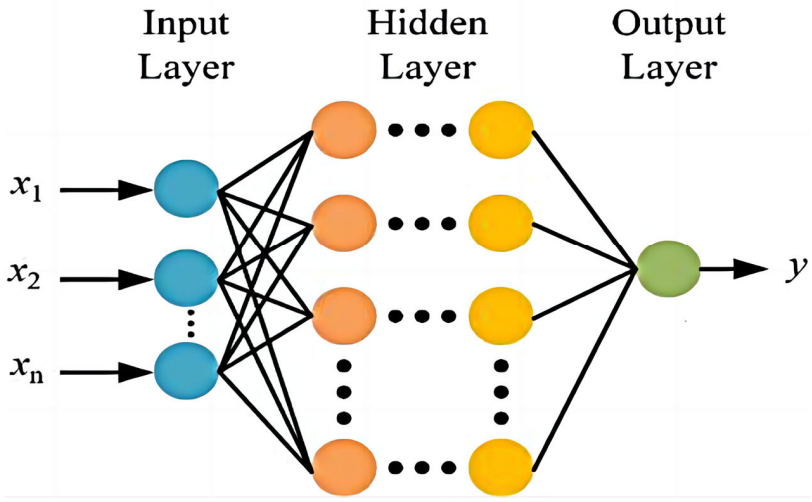


Figure 6. Schematic of ANN.

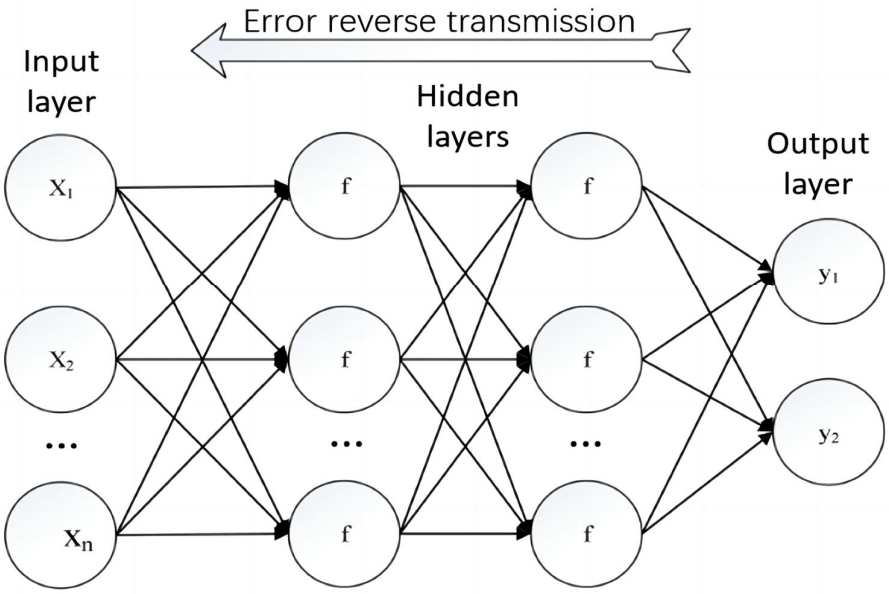


Figure 7. Error back-propagation example diagram [26].

3.2. Support Vector Machine Model

The support vector machine (SVM) model shows many unique advantages in solving small-sample, nonlinear, and high-dimensional pattern recognition problems and can be extended to other machine learning problems such as function fitting. The SVM helps to classify data by creating hyperplanes that act as margins to separate sets of data, as shown in Figure 8. After continuous improvement, a support vector machine regression (SVR) model was later proposed and used widely. In the SVR model, there is one training sample set as $\{(x_i, y_i), i = 1, 2, \ldots, n\}$, where $y_i \in R$ is the output value, and the d-dimensional vector $x_i = [x_{i1}, x_{i2}, \ldots, x_{id}]^T$ represents the i_{th} input [27]. Let the linear regression function be $f(x)$:

$$f(x) = \omega\varphi(x) + b \tag{2}$$

where $\varphi(x)$ is a nonlinear mapping function, and ω and b are the parameters to be solved. In the process of SVR training, in order to ensure the existence of support vectors and reduce the impact of abnormal data on the model, the insensitive loss function ε and relaxation

variables ξ_i and ξ_i* are introduced. The following equation is used to modify the constraints and optimization objectives of the function:

$$\begin{cases} \min \frac{1}{2}\|\omega\|^2 + C\sum_{i=1}^{l}\left(\xi_i + \xi_i^*\right) \\ s.t. \begin{cases} y_i - \omega\varphi(x_i) - b \le \varepsilon + \xi_i \\ -y_i + \omega\varphi(x_i) + b \le \varepsilon + \xi_i^* \\ \xi_i \ge 0 \\ \xi_i^* \ge 0 \end{cases} \end{cases} \tag{3}$$

where ε is an empirical value; the calculation is executed when the error of the actual y_i and the output of $f(x_i)$ is greater than ε, thus allowing the existence of a certain error; and a smaller ε value indicates that the regression equation in the error requirements is smaller. Additionally, C is the penalty factor, which specifies the cost of the sample points with errors greater than ε, and a larger C value indicates that the regression equation does not allow the existence of error points. In order to simplify the calculation by introducing the kernel function to complete the nonlinear transformation, the above equation is transformed to solve the k and k* pairwise problem:

$$\begin{cases} \max\left[\sum_{i=1}^{n}(k_i - k_i^*)Y_i - \frac{1}{2}\sum_{i=1}^{n}\sum_{j=1}^{n}(k_i - k_i^*)(k_j - k_j^*)K(X_i, X_i) - \sum_{i=1}^{n}\left(k_i + k_i^*\right)\varepsilon\right] \\ s.t. \begin{cases} \sum_{i=1}^{n}\left(k_i - k_i^*\right) = 0 \\ 0 \le k_i \le c, 0 \le k_i^* \le c \end{cases} \end{cases} \tag{4}$$

where the radial basis kernel function formula is expressed as:

$$K(X_i, X_j) = \exp\left(-g\left\|X_i - X_j\right\|^2\right), g > 0 \tag{5}$$

Here, g is the variance of the radial basis kernel function, a parameter that also has a large impact on the accuracy of the model.

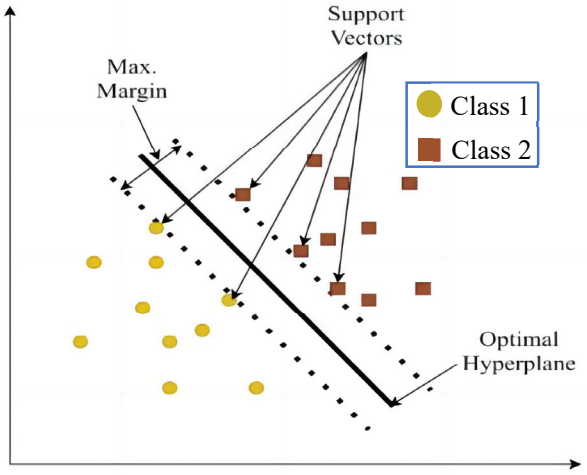


Figure 8. Schematic diagram of SVR model [27].

Even though the SVM has good generalization performance, because its implementation involves approximation algorithms based on the high complexity of time and space, the classification results of actual applications of the SVM are often far below the level expected in theory. The optimization of the finite classification performance of real SVM models can be achieved using SVM integration with bagging (bootstrap aggregation) or boosting. The SVM ensemble, whose general architecture is shown in Figure 9, is recommended.

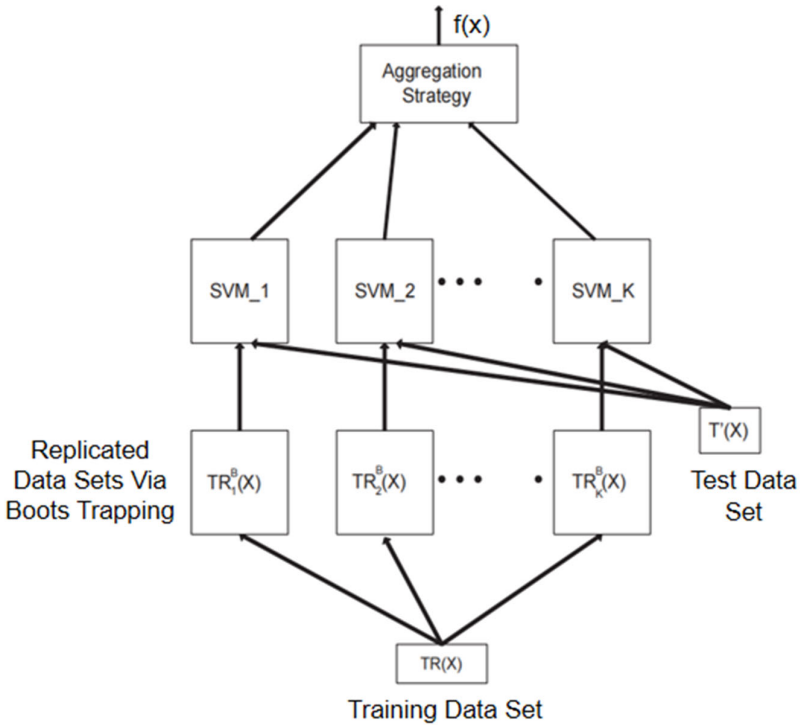


Figure 9. General architecture of the SVM ensemble [28].

After training, several independently trained SVMs need to be aggregated in an appropriate manner, such as linear or nonlinear combinatorial methods. For the C-class classification problem, there are two kinds of extension according to the insertion level of the SVM ensemble: (1) binary-class-level SVM ensembles (see Figure 10), and (2) multi-class-level SVM ensembles (see Figure 11).

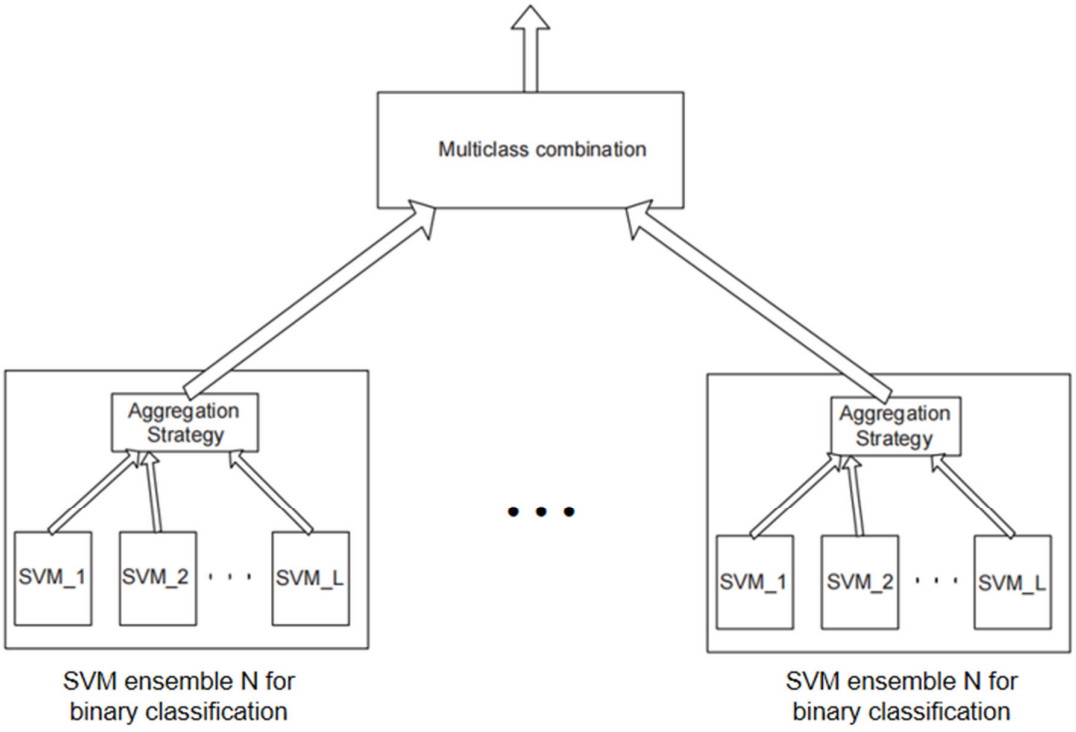


Figure 10. Binary-class-level SVM ensemble [28].

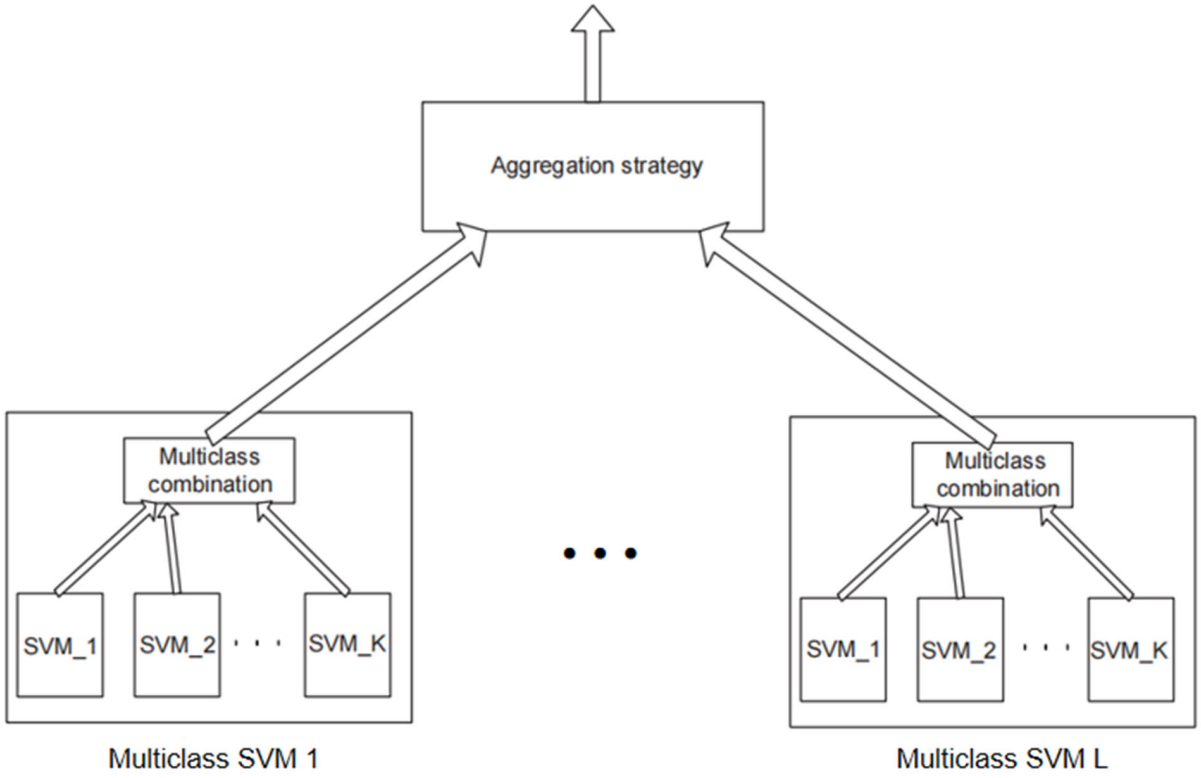


Figure 11. Multi-class-level SVM ensemble [28].

3.3. Random Forest Model

Integrated learning methods, as a prominent branch of machine learning, are capable of effectively overcoming the inherent limitations of individual models. By integrating diverse base models, these methods can complement each other and thus form a more powerful and versatile model. This approach helps to avoid the constraints and limitations that may arise from relying on a single model. Random forest is an algorithm that integrates multiple decision trees to predict the final outcome through the idea of integrated learning. This method is considered one of the most powerful machine learning algorithms due to its fast training speed, low computational expenses, and high accuracy. Random forest has been utilized in numerous practical applications due to its effectiveness. The random forest approach combines a bagging algorithm and a multilevel decision tree; the formation process of a random forest is depicted in Figure 12. A decision tree consists of nodes and directed edges, where the nodes include a root node (box), internal nodes (circle) and leaf nodes (triangle). The root node represents the example space itself, the internal node represents a feature or attribute, and the leaf node represents a specific category.

Table 1 shows some of the parameters involved in the random forest model. Each parameter in the model has a certain influence on the fitting performance of the final random forest model. The parameters n_estimators, max_depth, and max_features have a more important influence on the fitting accuracy of the model. Thus, when performing parameter tuning for a random forest model, the above three parameters are selected for tuning and optimization in order to improve the fitting performance of the final model.

3.4. Intelligent Optimization Algorithms

Drawing inspiration from human intelligence, the social dynamics of biological groups, and the laws of natural phenomena, numerous intelligent optimization algorithms have been developed to tackle intricate combinatorial optimization problems. These algorithms include genetic algorithms that emulate the evolutionary mechanisms of organisms in nature, ant colony algorithms that replicate the collective path-finding behavior of ants, particle swarm algorithms that simulate the group behavior of flocks of birds and schools

of fish, simulated annealing algorithms that stem from the annealing process of solid matter, and the gray wolf optimization algorithms that emulate the leadership and hunting hierarchy of gray wolves in nature.

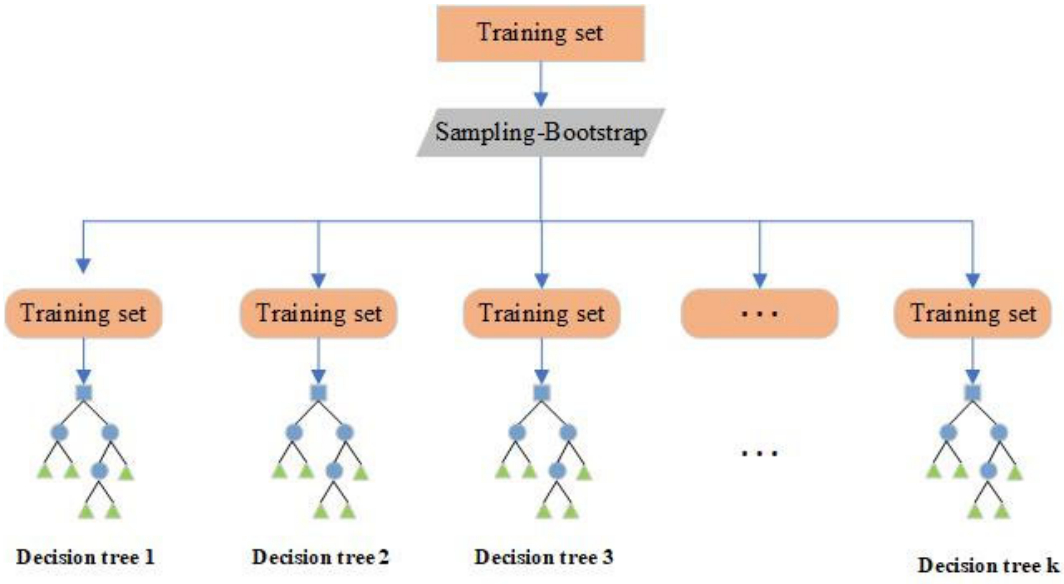


Figure 12. Schematic of the random forest formation process.

Table 1. Random forest model parameters.

Parameter	Meaning
n_estimators	Number of decision trees in the random forest
max_depth	Maximum depth of decision tree
max_leaf_nodes	Overfitting can be prevented by limiting the maximum number of leaf nodes
min_samples_leaf	Minimum number of samples of leaf nodes
class_weight	Sample category weights
min_weight_fraction_leaf	The minimum value of the sum of the leaf node sample weights
min_impurity_split	Limits the growth of the decision tree
max_features	The number of feature divisions in the selection of the most suitable attribute cannot exceed this value

4. Applications

4.1. Neural Networks

Neural networks are an intersection of machine learning and biological sciences that mimic the way biological neurons and brains process data. Neural networks can identify and learn the changing relationships between input and output data, and well-trained neural network models are widely used to predict data outcomes in many engineering applications. Meanwhile, in pursuit of better fitting and prediction performance, many researchers have proposed various types of neural networks, such as convolutional neural networks (CNNs) and recurrent neural networks (RNNs) [29–31]. The application of neural networks in fuel cells mainly includes the design of fuel cell components, the prediction of fuel cell performance and durability, and the design of fuel cell systems and vehicles.

Regarding the application of neural networks in the design of fuel cell components, Pourrahmani et al. [32] analyzed the factors affecting convective heat transfer in PEMFCs and employed an ANN model to conduct sensitivity analysis on each influential factor. The ANN model utilized a weight vector to demonstrate the extent of the influence of each input parameter on the output quantity. The results showed that the maximum error value of the ANN model prediction was approximately 0.0157, indicating a high level of accuracy

for the model. To summarize, the study effectively investigated the influential factors of convective heat transfer in PEMFCs and produced reliable results through the ANN model. Ahadian et al. [33] employed an ANN model to forecast the impact of various structural parameters on the cathode CL (CCL)'s activation overpotential in PEMFCs. The model inputs comprised platinum and carbon mass loads, GDL volume fraction, CCL thickness, GDL porosity, and membrane volume fraction in the CCL, while the output was the activation overpotential of the CCL. The ANN model's accuracy was evaluated using the root mean squared error (RMSE), which yielded an average RMSE of 7.20×10^{-4}, attesting to the superior predictive capabilities of the ANN model in simulating the activation overpotential as a function of the input parameters.

Hwang et al. [34] proposed a novel technique that integrated image-based embodiment-based characterization and a deep learning ANN for the quantitative analysis of multiphase microstructures of SOFC cathode composites. The approach was validated using FIB-based image data, which combined a focused ion-beam-based SEM analysis procedure with the automatic slicing of the focused ion beam method. Deep learning algorithms were employed to analyze SOFC microstructures, such as the volume fraction, interconnectivity, and multiphase boundaries. The study utilized 49 FIB-extracted SE images, 40 of which served as the training set and 9 as the test set, to assess the reliability of the algorithm. The successful application of the semantic segmentation-assisted deep learning algorithm for the microstructural analysis of multiphase composite electrodes indicated that it could be extended to similar multiphase mixtures, leading to a significant reduction in analysis time and improved image summaries. The flow is shown in Figure 13. Liu et al. [35] developed a deep learning accelerated homogenization framework for predicting the elastic modulus of porous materials directly from their internal microstructure, and the framework construction process is shown in Figure 14. A CNN was built on the foundation of a large amount of simulation data.

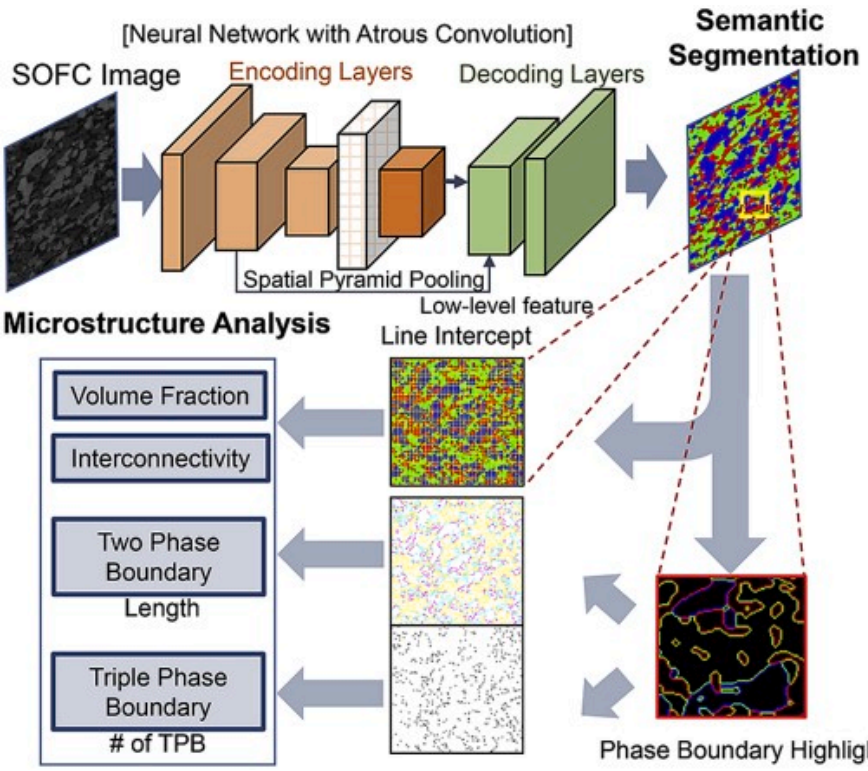


Figure 13. Strategy utilizing DL to assist in the application of semantic segmentation for quantitative microstructure analysis in solid oxide fuel cells [34].

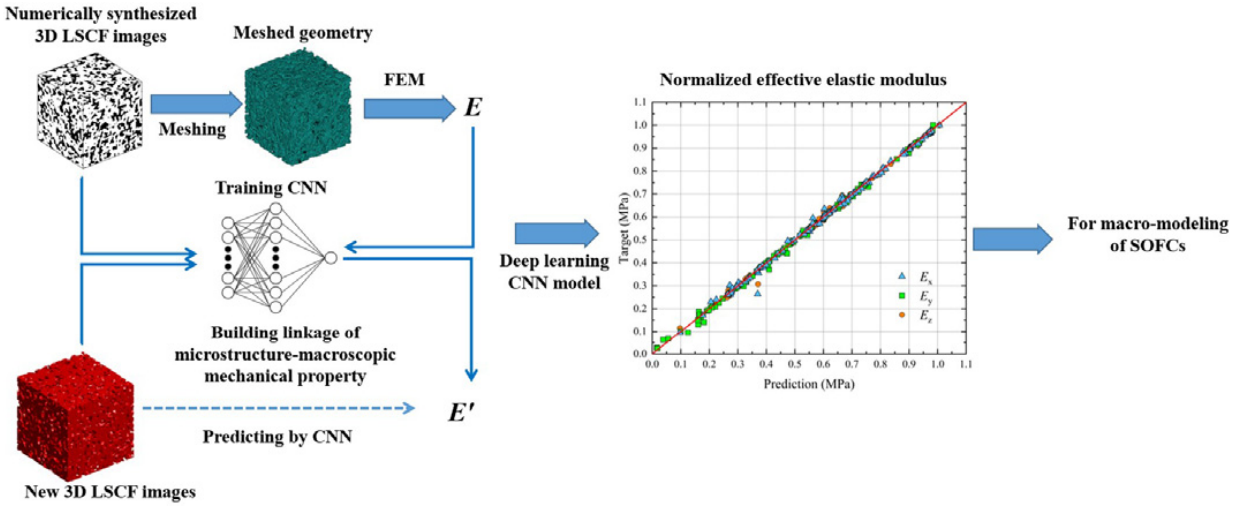


Figure 14. Using the DL and FEM methods, the elastic modulus of a porous LSCF cathode is predicted based on its internal microstructure [35].

Regarding the application of neural networks in the prediction of fuel cell performance, Khajeh et al. [36] employed BP neural network techniques to predict the performance of the catalytic layer in a fuel cell. The neural network model was developed successfully and combined with statistical methods to determine the most significant cell variables impacting the catalytic layer's performance. Seyhan et al. [37] used a feedforward network consisting of a multilayer perceptron with two hidden layers to model the relationship between the operating parameters of a PEMFC and the current, and the Levenberg–Marquardt training algorithm was used as an error back-propagation method. The study was conducted on a PEMFC with a sinusoidal serpentine flow channel, and the fuel cell performance was first measured experimentally under different cell temperatures, gas flow rates, and channel amplitudes. Then, the neural network model was trained and tested with different channel amplitudes, hydrogen and air flow rates, cell temperatures, and input voltages as input variables, and the cell current as the output variable. This showed that the prediction results of the developed neural network model were comparable to the experimental results. The neural network model not only reduced the number of experiments but also predicted the optimal operating conditions of the PEMFC within the range of input parameters. The structure of the conventional BP neural network used by the authors is shown in Figure 15 and the number in the input layer indicates the number of neurons in that layer, which is the number of inputs.

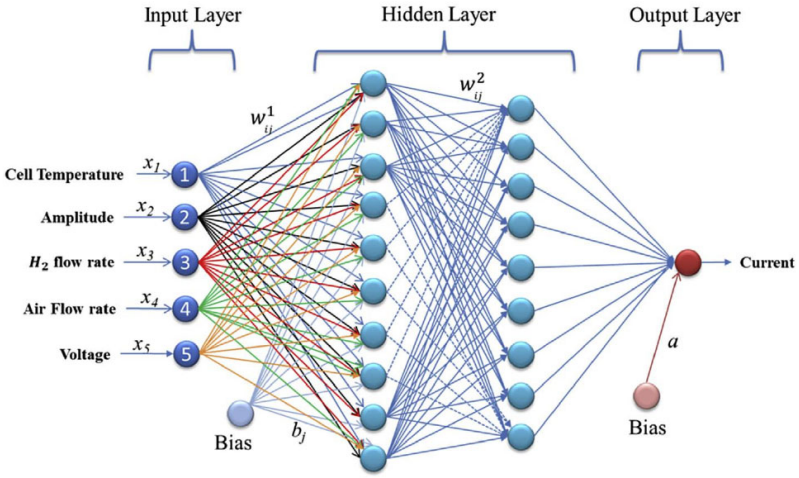


Figure 15. Schematic diagram of traditional BP neural network structure [37].

Lopes et al. [38] proposed a system identification modeling approach based on a nonlinear autoregressive network with exogenous input (NARX) and nonlinear output error (NOE) neural network to build a black box model for predicting the output performance of a PEMFC power stack. The model inputs were current and past voltage, and the output was the present voltage. The final results showed that the proposed model could provide highly accurate predictions of the stack voltage over extended periods of time. Both neural networks could well approximate the time-varying behavior of the PEMFC power stack without having to retrain the network for a long time. Additionally, the models had fewer hidden layer neurons and smaller regression vectors, which worked well over the entire operating range of the PEMFC stacks. He et al. [39] used a back-propagation neural network (BPNN) and an adaptive neuro-fuzzy inference system to predict the effects of the operating parameters and the historical states of the PEMFC on the future performance of the PEMFC, respectively. The degree of influence of the historical states and operation mode on the future performance of the PEMFC under different operating scenarios was compared. The input variables of the BPNN were time, inlet temperature, and inlet pressure, and the output variable was cell potential. The results could help to select more suitable parameters for the prediction of PEMFC performance in practical PEMFC applications and achieve high prediction accuracy under complex operating conditions. Lee et al. [40] constructed a BP neural network containing a single hidden layer to predict the potential of a proton exchange membrane fuel cell. The results showed that the predicted potentials agreed well with the experimental data, with an error of no more than 0.25%, indicating that the neural network approach could be successfully used for the study of fuel cell modeling. Saengrung et al. [41] constructed and compared two different neural networks, a BP neural network and a radial basis neural network, to explore the effect of varying the number of neurons and hidden layers. The results showed that both neural networks could successfully predict the stack voltage and current of fuel cells, and the method was very suitable for the real-time control of the cells in engineering practice. Napoli et al. [42] applied a conventional neural network to construct a data-driven model of a fuel cell, which was designed to predict the stack voltage and temperature of the cell under dynamic conditions, and the results showed that the model had a high prediction accuracy. Marra et al. [43] built a neural-network-based predictor for solid oxide fuel cells and discussed the training process as well as the selection of model input parameters, and the results showed that the built intelligent predictor could accurately predict the real-time voltage of the cell. Jian et al. [44]. used a genetic algorithm to optimize the weight parameters of a BP neural network in order to construct an output voltage prediction model for fuel cell vehicles. The optimized neural network prediction results were compared with the experimental results. This showed that the maximum relative error between the predicted value and the actual output value of the network never exceeded 5%. Dang et al. [45] used deep learning methods for the fault diagnosis of fuel cells. The convolutional neural network technique was used to determine the possible water management, hydrogen leakage, and other unexpected conditions in the battery operation. The superiority of their proposed diagnostic technique was demonstrated by comparing it with intelligent learning algorithms such as the K-neighborhood algorithm and support vector machine.

Bicer et al. [46] investigated the use of neural network techniques to model a smart grid containing PEMFCs. After the network was successfully trained and validated, it was applied to analyze the dynamic behavior of the grid. Wang et al. [47] used a BP neural network approach to develop a steady-state performance prediction model and a dynamic performance prediction model for a high-temperature PEMFC, respectively. The training data of the neural network were obtained from the cell voltages measured under different operating conditions, and the operating pressure, temperature, and cathode gas type of the cell were used as input variables to achieve the accurate prediction of both the steady-state and dynamic performance of the high-temperature PEMFC in a Matlab/Simulink environment. Yan et al. [48] used a CFD method to simulate the operation of a single cell and calculated the corresponding current density values by varying the runner heights

and widths, and a neural-network-based integrated learning model was constructed as the the base learner for bagging based on these CFD simulation data. By comparison with the BP neural network, it was found that the bagging–neural network integrated model could be used with only a small amount of training data. The proposed method was a good solution to the current training problem in PEMFCs related to the difficulty of obtaining training data. Barzegari et al. [49] obtained a dynamic data-driven model for cascaded PEMFC stacks using a neural network approach, which was validated with experiments showing that the mean square error of the model prediction was less than 3%. Tsompanas et al. [50] applied neural networks to model the polarization curves of microbial fuel cells using different material membranes. A conventional BP neural network was used, and the correlation coefficient of the predictions was 0.99662, indicating that the BP neural network had good accuracy in predicting the cell voltage. Laribi et al. [51] and Arama et al. [52] used a neural network approach to solve the water management problem in fuel cells, and the results of both studies showed that the neural network model could control the hydration characteristics of the cell well. Guo et al. [53] applied an Elman neural network combined with optimization methods to identify some unknown parameters in the mathematical model of a fuel cell. By comparing the cell polarization curves identified by the Elman network with experimental data, it was shown that the network could successfully predict the cell potential under different operating conditions. Morando et al. [54,55] successfully used echo state networks to predict the aging characteristics of PEMFCs at a constant current. Khajeh et al. [36] presented a mathematical surrogate method that combined a physical model of the cathode CL (CCL) and an ANN model. This approach was developed to accurately forecast the performance of the CCL in a PEMFC, specifically the activation overpotential (η-act), as illustrated in Figure 16.

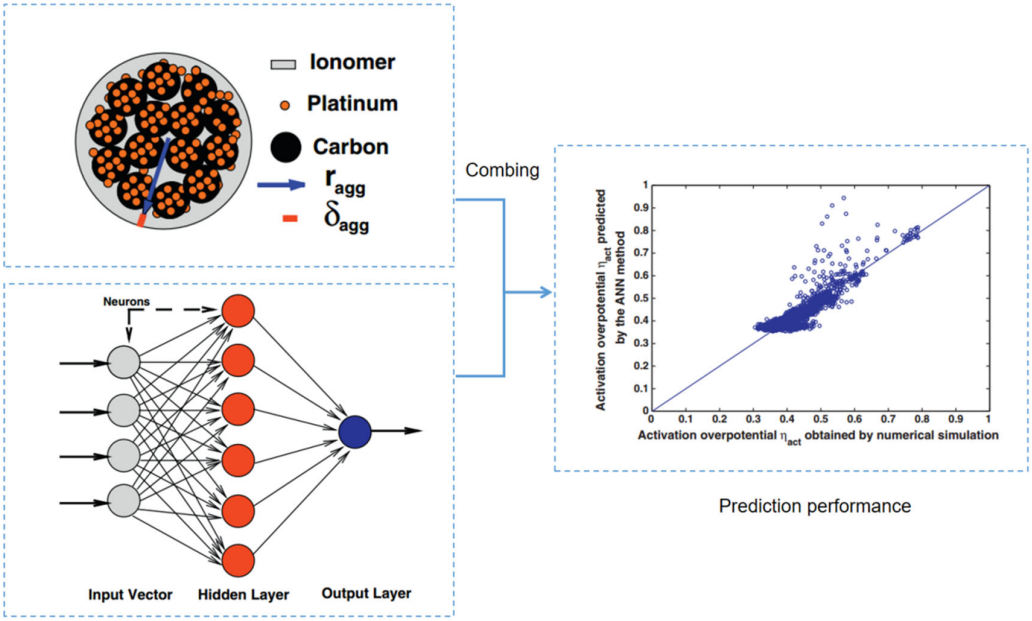


Figure 16. Prediction of the CCL performance of a PEMFC based on the combination of a CCL physical model and ANN model [36].

In the case of the structural optimization of flow channels, the traditional method of flow channel optimization is the controlled variable method, in which a single factor is gradually varied within a certain range, and each case is simulated or tested to obtain the variation law of the performance [56–59]. However, the traditional method is time-consuming in terms of calculations, the experiments are expensive, and it cannot consider the joint effect of different parameters; conversely, machine learning is an efficient and convenient method with lower costs. Yan et al. [48] utilized a three-layer bagging neural network model to investigate how the height of the inlet and outlet of the flow channel

impacted the output performance. The flow channels were classified as rectangular equal-section, tapering, and asymptotic expansion, depending on the combination of inlet and outlet heights. This approach was characterized by its ability to make fast predictions using minimal data, while also exhibiting good robustness. Pourrahmani et al. [60] optimized the bottom edge, top edge, and block arrangement spacing of the trapezoidal block from the heat transfer point of view, taking the Nu number and friction factor as the evaluation results. Using the results of the simulation, the ANN model was trained to optimize and calculate the best combination of structural parameters of the trapezoidal block for optimal heat transfer and minimum friction loss. The authors also optimized the DC channel embedded with seven arc-shaped blocks [61] and established 30 sets of block distribution conditions with different tilt angles, inlet distances, and heights, obtaining the corresponding Nu numbers and friction rates by simulation. The results were used to train the ANN model for big data analysis and sensitivity analysis, and it was found that the height of the first block at the entrance had the greatest effect on the heat transfer performance. Similarly, a DC channel embedded with four uniformly distributed rectangular blocks was designed by Li et al. [62], in which the height of the four blocks gradually increased. The authors used the entrance block height and height increment as variables and the cell performance as the evaluation index. The final optimization results showed that the best performance was achieved with an entrance block height of 0.9537 mm and an increment of 0.009 mm. Guo et al. [63] used ANN to optimize the block structure parameters of PEMFC novel block channels including the length, width, and height of the block. The datasets were obtained from a three-dimensional two-phase flow model [64], with the computational domain of the two-block channel shown in Figure 17. The block length is L, the height is H, and the width is W. These three parameters were the optimization objectives.

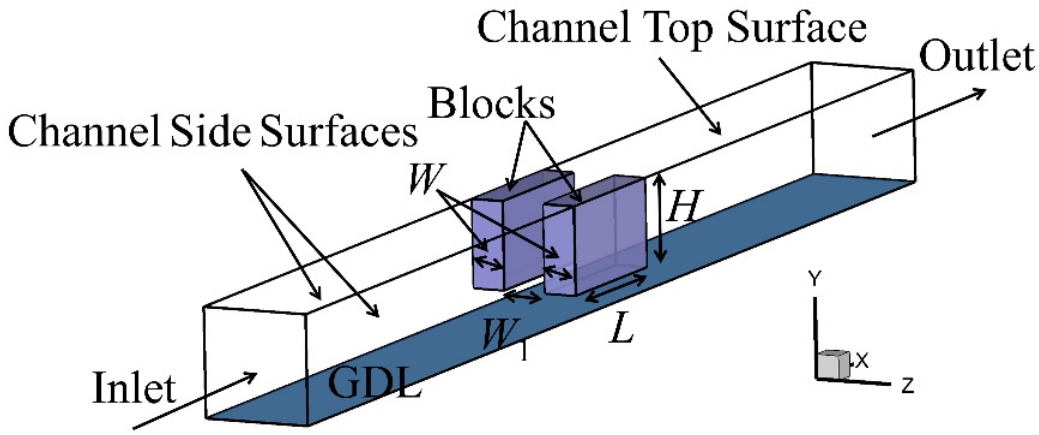


Figure 17. Computational domain of the two-block channel [63]. The channel length is 12 mm, and the cross-section is 1 mm × 1 mm.

The training/test datasets were obtained from a three-dimensional multi-phase model based on the volume-of-fluid (VOF) method, with the water removal time (T) and the maximum channel pressure drop (ΔP) taken as the output and optimization objectives. Forty-three datasets were collected from the physical model and randomly split into test and training sets in a 7:3 ratio (Figure 18). The datasets included measurements for block height (H), block width (W), gap width between blocks (W_1), and block length (L).

Figures 19 and 20 indicate the good fitting results of the ANN model. Figure 19 illustrates the correlation between the predicted values of the ANN model and the actual values of the physical model. Figure 20a demonstrates the relative error of ΔP for the simulation cases, and Figure 20b shows the relative error of T for the simulation cases.

Cases	H (mm)	W (mm)	W_1 (mm)	L (mm)	T (ms)	ΔP (Pa)
Case 1	0.7	0.3	0.4	1.4	13.32	128.43
Case 2	0.8	0.3	0.4	1.4	7.86	210.06
Case 3	0.85	0.3	0.4	1.4	7.86	250.07
Case 4	0.9	0.3	0.4	1.4	7.92	300.12
Case 5	1	0.3	0.4	1.4	8.46	322.88
Case 6	0.8	0.475	0.05	1.4	15.2	1933.04
Case 7	0.8	0.45	0.1	1.4	8.1	1305.08
Case 8	0.8	0.4	0.2	1.4	7.43	609.83
Case 9	0.8	0.35	0.3	1.4	7.61	332.71
Case 10	0.8	0.25	0.5	1.4	13.73	118.65
Case 11	0.8	0.3	0.4	0.1	13.8	142.89
Case 12	0.8	0.3	0.4	0.2	8.73	140.96
Case 13	0.8	0.3	0.4	0.5	7.94	199.47
Case 14	0.8	0.3	0.4	1	7.86	204.21
Case 15	0.8	0.3	0.4	2	7.86	221.37
Case 16	0.8	0.3	0.4	2.5	7.86	223.27
Case 17	0.725	0.475	0.05	0.3	8.23	683.21
Case 18	0.775	0.425	0.15	0.95	7.49	713.67
Case 19	0.7	0.25	0.5	1.25	14.23	96.3
Case 20	0.75	0.375	0.25	0.6	7.58	301.1
Case 21	0.675	0.4	0.2	0.475	7.76	246.43
Case 22	0.9	0.275	0.45	1.55	8.39	233.01
Case 23	0.975	0.45	0.1	0.8	7.77	612.18
Case 24	0.8	0.35	0.3	0.75	7.59	313.41
Case 25	0.85	0.375	0.25	1	7.57	637.35
Case 26	0.925	0.325	0.35	1.3	7.75	421.7
Case 27	0.825	0.275	0.45	1.1	13.38	142.76
Case 28	0.875	0.3	0.4	1.5	7.88	275.86
Case 29	0.95	0.35	0.3	0.725	7.77	612.18
Case 30	0.85	0.3	0.4	2.1	7.85	270.24
Case 31	0.95	0.275	0.45	0.225	13.9	164.62
Case 32	0.7	0.375	0.25	0.775	7.73	236.42
Case 33	0.8	0.375	0.25	0.775	7.53	411.34
Case 34	0.65	0.375	0.25	0.8	12.8	161.85
Case 35	0.675	0.3	0.4	1	13.72	112.44
Case 36	0.675	0.45	0.1	0.9	11.26	372.1
Case 37	0.65	0.275	0.45	0.8	14.35	92.93
Case 38	0.625	0.325	0.35	0.7	13.83	109.92
Case 39	0.75	0.35	0.3	0.4	7.67	231.37
Case 40	0.725	0.375	0.25	0.325	7.68	243.82
Case 41	0.725	0.325	0.35	1.2	12.88	155.91
Case 42	0.75	0.3	0.4	1.6	12.93	153.79
Case 43	0.775	0.275	0.45	2	13.03	146.24

Figure 18. Simulation cases and results [64].

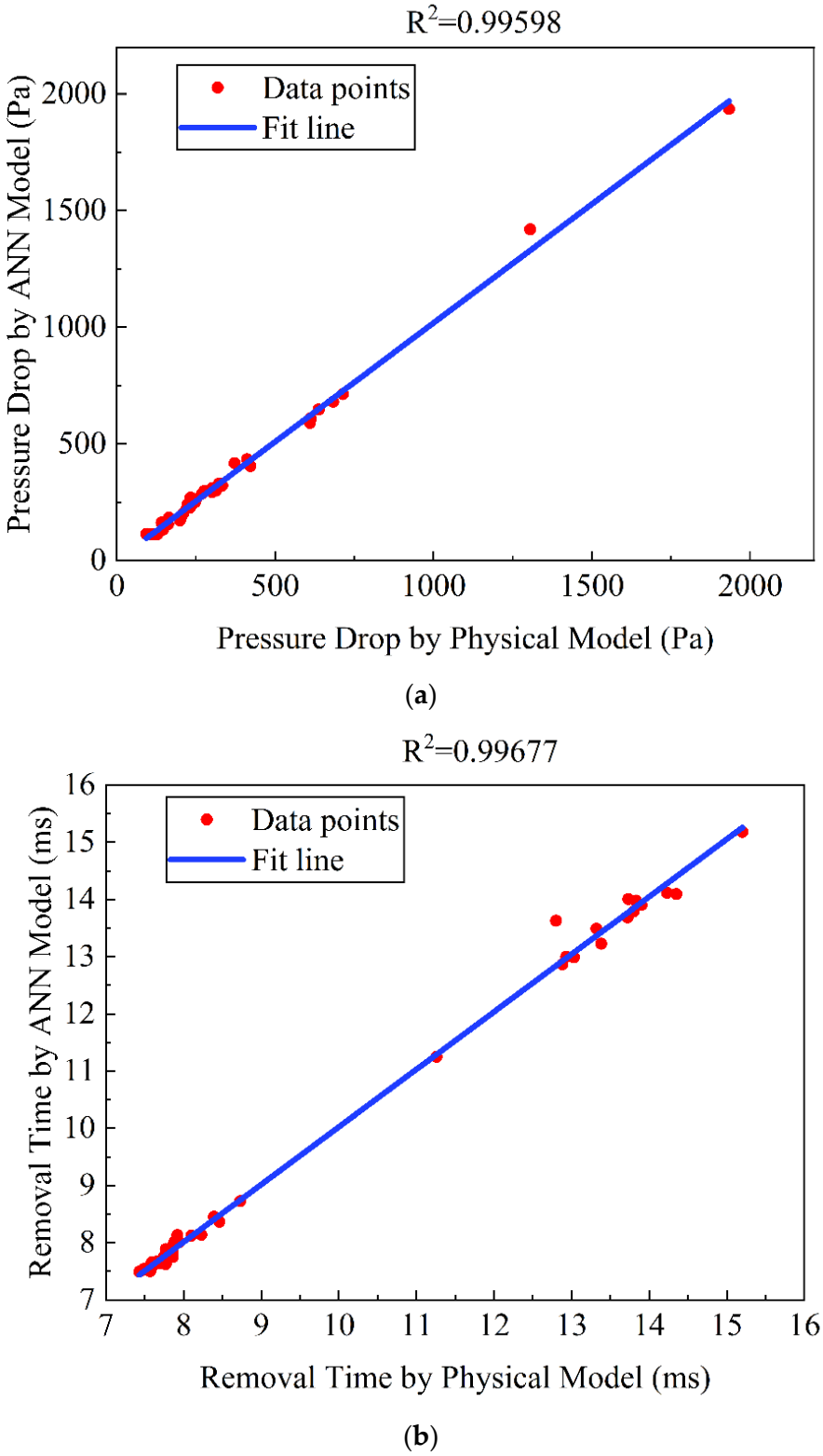


Figure 19. Small R^2 values for pressure drop (**a**) and water removal time (**b**) were achieved by the ANN model [63].

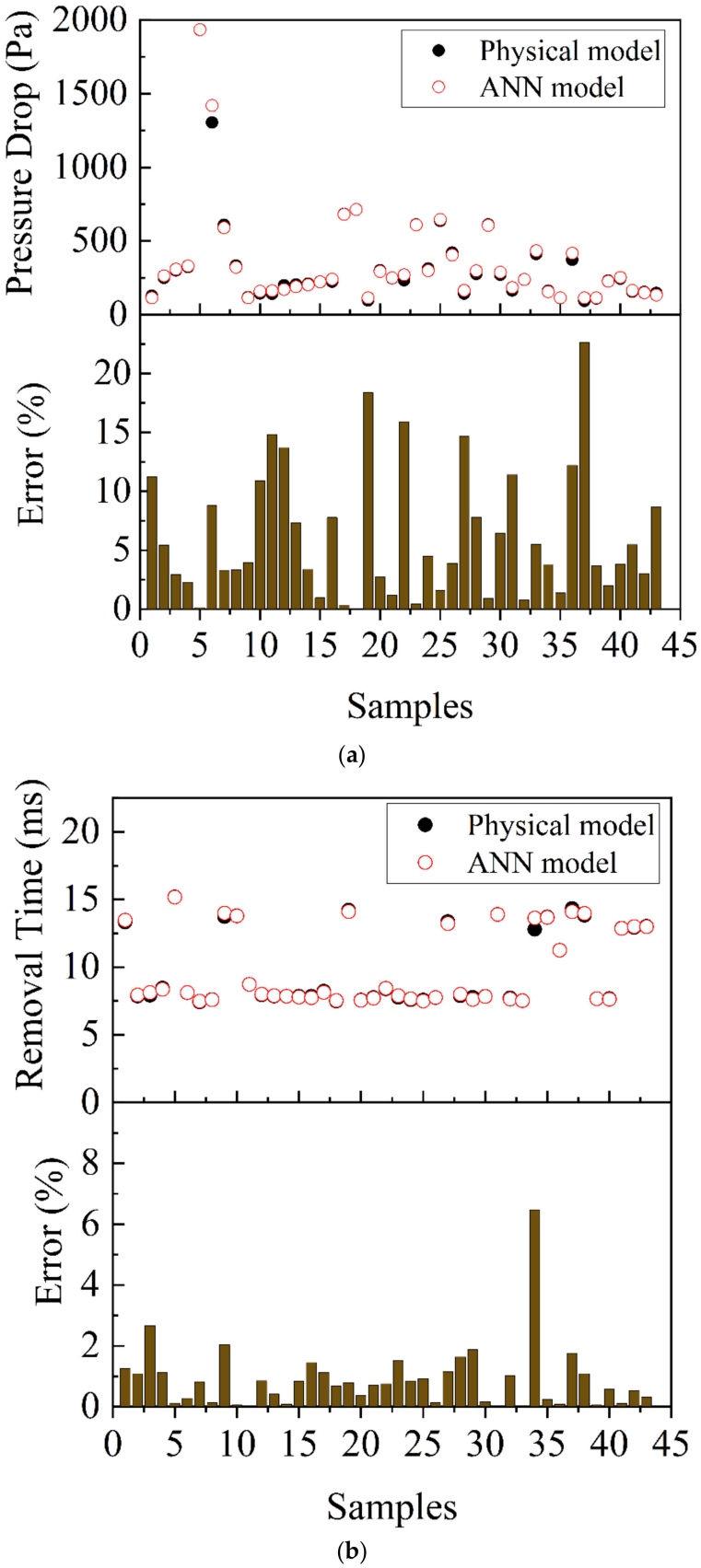


Figure 20. Small relative errors for pressure drop (**a**) and water removal time (**b**) predictions were achieved [63].

The block parameters were further optimized using a comprehensive scoring method considering both T and ΔP. The block parameters with a length of 0.8 mm, width of 0.375 mm, and height of 0.75 mm were found to achieve the highest score.

Regarding the application of neural networks in the prediction of fuel cell durability, Yang et al. [65] proposed a degradation prediction method for PEMFCs that utilized multivariate polynomial regression (MPR) and an ANN to analyze data and accurately forecast short-term degradation behavior. This approach was driven by data and provided a reliable solution for predicting PEMFC degradation. The study trained the model based on the degradation data of the PEMFC in both dead-ended anode (DEA) and anode recirculation modes. The proposed model aimed to characterize the degradation patterns of PEMFCs through a two-stage approach. Firstly, the initial cell performance was predicted using MPR. Secondly, the changes in cell performance over time were forecasted through the ANN. The input parameters of the ANN model were the operating voltage, inlet pressure, and time, and the output parameter was the current density. The results showed that the model combining MPR and ANN produced more accurate results than MPR or ANN alone, and the dual-hidden-layer neural network also demonstrated better prediction performance than the single-hidden-layer neural network. The mean and maximum relative errors of the dual-hidden-layer M-ANN model were 0.122 and 0.444, respectively. This was the method with the best prediction performance. Zuo et al. [66] combined an attention-based RNN model with prognostics and health management (PHM) to improve the predictive capability of PHM and its accuracy in predicting the output voltage decay of PEMFCs. The model was trained and tested based on long-term dynamic loading cyclic durability test data with input variables of time, load, etc., and an output variable of decay voltage. The results showed that the attention-based RNN model had higher prediction accuracy than PHM in fuel cell systems. Ma et al. [67] and Wang et al. [68] utilized S-LSTM and G-LSTM, respectively, to forecast the residual lifespan of PEMFC systems.

Regarding the application of neural networks in the fuel cell systems and vehicles, Jeme et al. [69] created a fuel cell vehicle power system using a neural network model of a PEMFC stack. The PEMFC stack parameters are shown in Table 2. The model's inputs included the current, partial pressures of hydrogen and oxygen, and stack temperature, while the output was the stack output voltage. The established model's prediction results were comparable to the experimental results, indicating the potential development of a control law for on-board energy conversion in fuel cell vehicles. Xu et al. [70] introduced a novel hybrid approach that integrated a multi-physics simulation (MPS) with deep learning to predict the crucial parameters of SOFCs that operate with intricate fuel compositions. The DNN algorithm was trained using a dataset derived from the MPS model, which accounted for electrochemical reactions, chemical reactions, mass/momentum transport (CFD), and heat transfer. Figure 21 illustrates a schematic of a SOFC with a complex fuel composition and a workflow that combines several physical models and artificial intelligence simulations.

Table 2. PEMFC stack parameters [69].

Parameter	Value
Number of cells, n	20
Activation area, A_{act}	2.0×10^{-4} m^2
Operating temperature range, T	20–60 °C
Operating voltage, V	12 V
Power, P	500 W

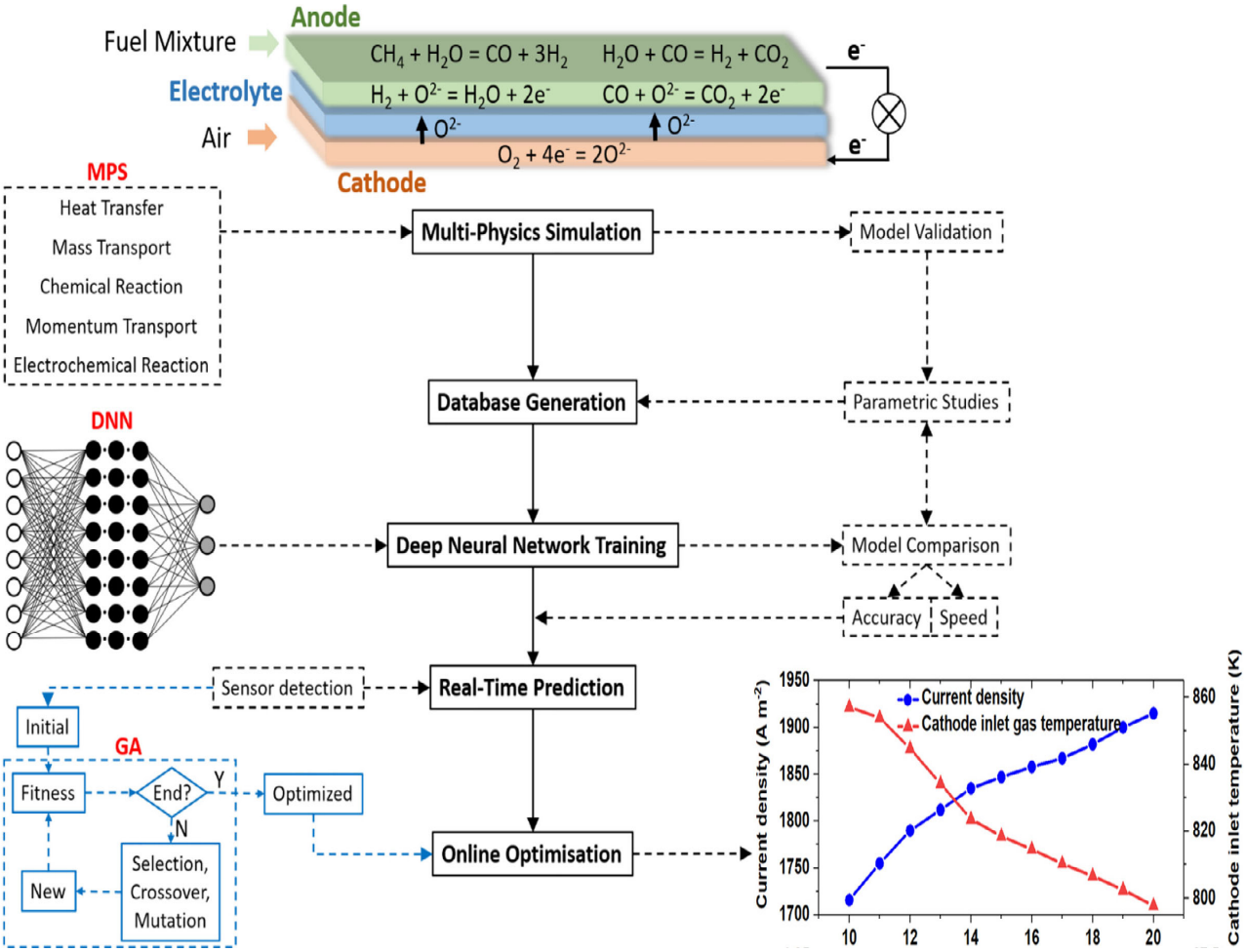


Figure 21. An SOFC schematic featuring intricate fuel composition and simulations driven by AI [70].

Many researchers have also compared neural networks with other machine learning methods for fuel cell applications. Legala et al. [71] modeled the PEMFC performance attributes and internal states based on two machine learning methods, ANN and SVR, respectively. The machine learning models were trained and tested using data obtained from semi-empirical models and experimentally validated 1D CFD model. The input variables for the machine learning model were operating conditions such as inlet pressure, gas flow rate, relative humidity, and cell temperature for both the cathode and anode, and the output variables were cell voltage, membrane resistance, and membrane hydration (water content). The results showed that the ANN had a significant advantage compared with SVR, especially in multivariate output regression. However, SVR did not require an excessive number of iterations, reducing the computation time without sacrificing accuracy for simple regression. Chauhan et al. [72] used three machine learning models (logistic regression, SVM and ANN) to identify the pressure drop in the flow channel of a PEMFC influenced by liquid water. The images of liquid water distribution in the flow channel were first obtained experimentally and then post-processed as input data for the machine learning models, which output different pressure drop ranges. Finally, the performance of the machine learning models was compared using a confusion matrix and classification accuracy. The results showed that ANN had the highest accuracy in predicting the pressure drop for two-phase flow. Han et al. [73] employed neural network and support vector machine (SVM) techniques to build two models. The hyperparameters of these models were determined using a ten-fold cross-validation method. The study revealed that the neural network model was more effective than the SVM model in forecasting the polarization curve of the fuel cell. To enhance the quality of the text, a plagiarism check was conducted.

4.2. Support Vector Machines

The SVM model is designed for binary classification, and it operates by mapping the feature vectors of instances to specific points in space. Its primary objective is to draw a line that can effectively distinguish two different types of points. This line is created with the aim of ensuring that it can accurately classify any new points that may arise in the future. SVM is particularly useful when dealing with small or medium-sized data samples, as well as nonlinear and high-dimensional classification problems.

Regarding relevant research on PEMFCs using SVM algorithm, Kheirandish et al. [18] obtained 9725 sets of data by conducting experiments on an electric bicycle powered by a PEMFC and used these data to train an SVM model. SVM and multilayer perceptron (MLP) were both employed for the purpose of performance prediction for a 250 W fuel cell system. The input parameters considered for this prediction were current density and temperature, while the output parameter was voltage. The result showed that the prediction and estimation of the PEMFC performance based on SVM was better than that of the MLP modeling method, because of the former's high accuracy, lack of prior knowledge of the PEMFC, and use of the structural risk minimization (SRM) principle. The determination coefficient of the SVM power and current curve prediction model was about 99%. The determination coefficient of the MLP model was about 97%. Zou et al. [74] analyzed the credibility and definition of the reliable working range of least squares support vector machine (LSSVM) when dealing with multiple load changes. A transient model based on LSSVM was preliminarily established, and the influence of the fuel cell system settings and external load behaviors on the transient model were studied using data from Simulink simulations verified by experiments. The authors found that the fuel cell system settings with dense sampling produced better model performance than sparse sampling intervals. Li et al. [75] proposed a nonlinear predictive control algorithm based on the LSSVM model. The LSSVM model with a radial basis function (RBF) kernel was used to establish a nonlinear offline model of a PEMFC, so as to realize the nonlinear predictive control of the device and lay a good foundation for the online control of a PEMFC system. Han and Chung [76] proposed a hybrid model by combining the SVM model with empirical equations, which was trained, tested, and verified using PEMFC experimental data. The empirical equations captured the main variation in cell voltage, while the SVM model compensated for small changes due to other operational variables. The hybrid model accurately predicted the polarization curves and made up for the shortcomings of the SVM model when predicting in the high voltage range. The model could predict the voltage of PEMFCs even with varying operating parameters. Peng et al. [77] proposed an optimal design of a PEMFC power density model based on the artificial intelligence method of SVM. The power density model results were in good agreement with the experimental data. Wang et al. [15] developed a novel ML framework, combining a 3D CFD model, SVM model, and GA, to optimize the CL of a PEMFC for maximum power density, as depicted in Figure 22.

Huo et al. [78] utilized SVM to classify various fuel cell faults with a training set of 350 samples and a test set of 50 samples, achieving 94% accuracy after optimization using the genetic algorithm. The process was visualized in a flow chart (Figure 23). Zou et al. [79] proposed a hydrogen leakage detection method based on SVM. The mass conservation equation was used to obtain the hydrogen leakage fault characteristics of a fuel cell engine, and the PSO algorithm was used to optimize the radial basis kernel function SVM to detect hydrogen leakage in the fuel cell engine. The results showed that the detection accuracy for the hydrogen leakage of a fuel cell engine based on SVM was higher than 90% under different driving conditions. This approach could be applied to detect hydrogen leaks in fuel cell engines and serve as a basis for developing other detection methods. Li et al. [22] used Fisher discriminant analysis (FDA) to extract features from a single cell voltage. Then, the extracted features were classified into various categories related to the health state using the spherical multi-class support vector machine (SSMSVM) classification method. Thus, a data-based diagnosis strategy for PEMFCs was proposed that could detect new potential

failure modes in the process. Li et al. [80] proposed a classification-based diagnosis strategy for PEMFC systems, depicted in Figure 24. The SVM classifier was trained offline using the training dataset, and the trained SVM model was used to process real-time data in the online phase. The diagnosis inference could be obtained based on the classification results and diagnosis rules. Huo [81] applied the modeling method of support vector machines to SOFC modeling and used a SVM with the radial kernel function to build a nonlinear model of the SOFC power stack. The model had good accuracy as well as a strong generalization capability, which could effectively avoid the problem of local minima and was very suitable for small-sample modeling in the field of nonlinearity.

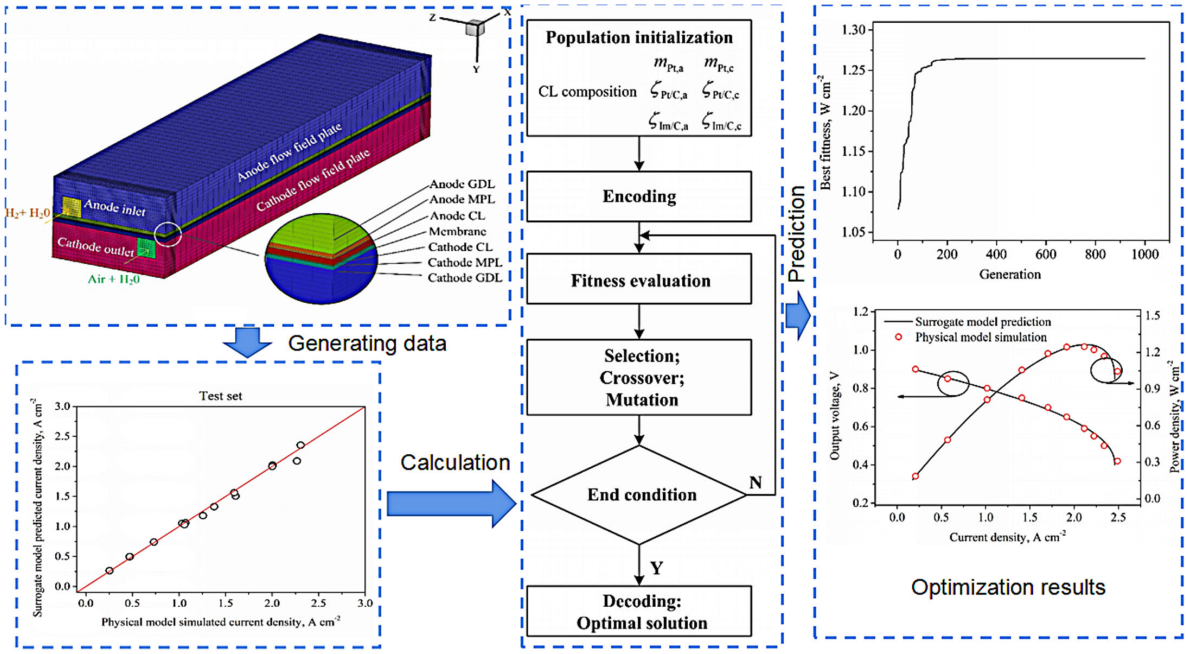


Figure 22. Optimization of CL for maximum power density in PEMFCs, achieved through the use of a 3D physical model and an ML model (SVM) [15].

4.3. Random Forest

Random forests (RFs) are a widely used ensemble learning technique with many applications in data mining and machine learning. Random forests are a nonparametric tree-based collective solution for effective data-adaptive inference that combines the notions of adaptive closest neighbors and bagging. The applications of random forests in PEMFCs mainly include catalyst preparation, cell performance prediction, fault diagnosis, and the rational design of the flow channel.

Elcicek and Özdemir [82] analyzed how synthesis process parameters affect fuel cell catalyst performance using statistical methods and RF. Many factors need to be considered to optimize catalyst performance, such as catalyst composition, morphology, and surface properties, as well as process parameters such as reaction conditions, reactant concentration, and reactant types. These factors interact to affect the performance of the catalyst. Using a comprehensive model to predict the optimization results, the interaction of these factors can be considered to improve the accuracy of the prediction. Huo et al. [83] used deep learning to design a performance prediction method based on the random forest algorithm and a CNN. Figure 25 illustrates that the weight parameters of the CNN-based performance prediction model were optimized using an optimization algorithm. This algorithm minimized the empirical loss function by calculating the difference between the predicted output and the target output of the model. In the proposed method, the random forest algorithm was used to select important factors as input features for the model in order to improve the quality of the training datasets.

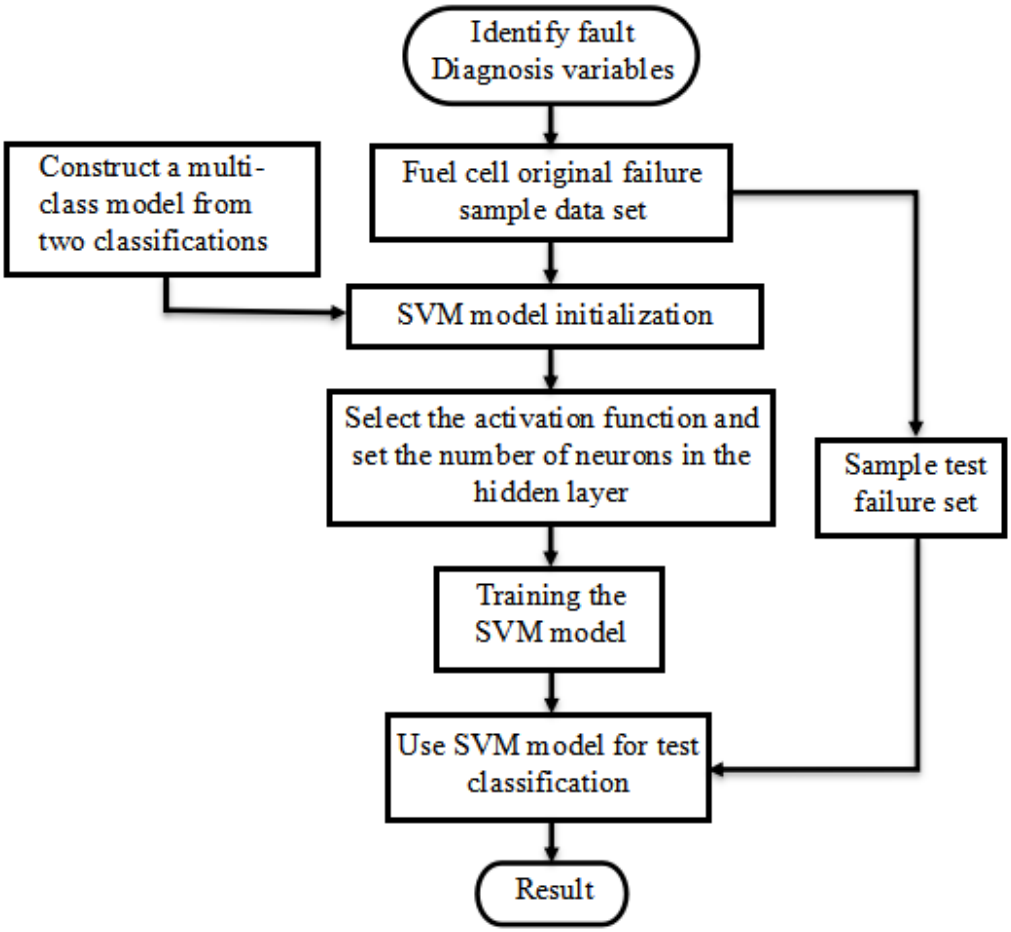


Figure 23. Flow diagram of the SVM diagnosis process [78].

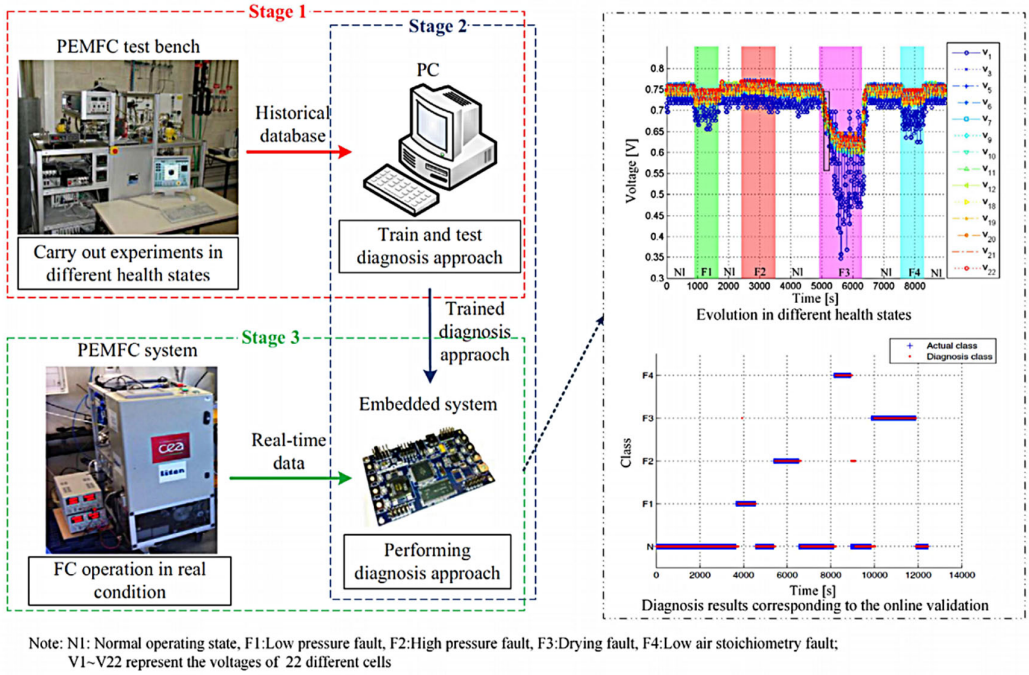


Figure 24. An online fault diagnosis approach based on SVM combined with the design of diagnostic rules for a PEMFC system [80].

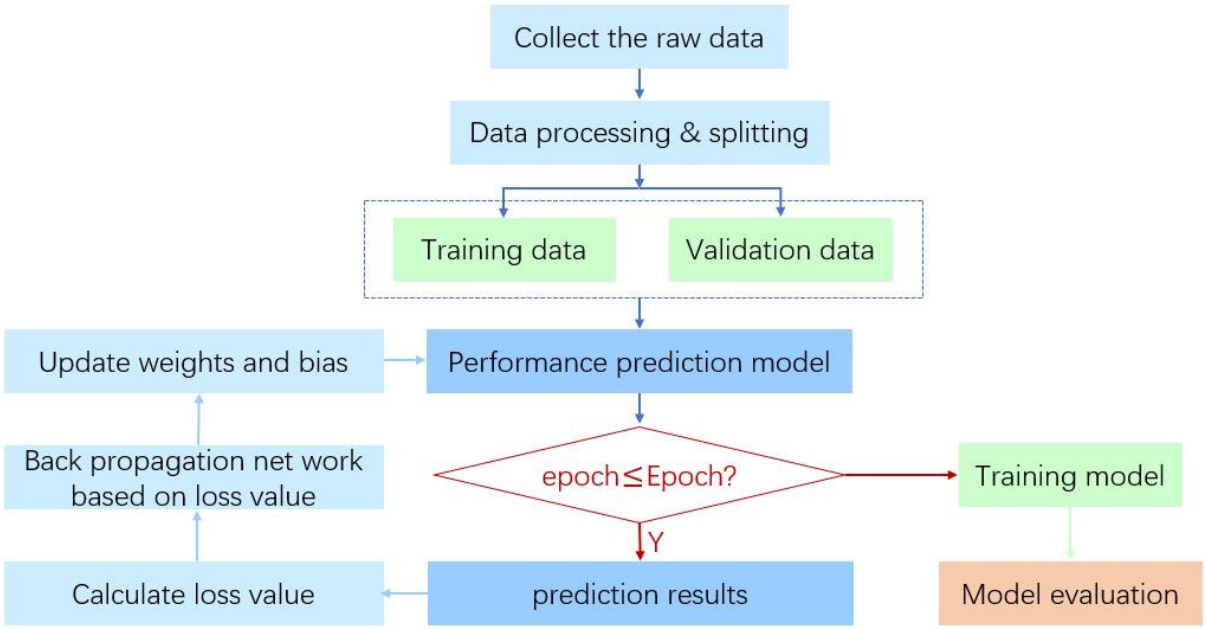


Figure 25. The training process of the performance prediction model [83].

In order to prevent the downtime of on-board fuel cell systems, Pang et al. [84] proposed an intelligent health state identification model for fuel cells under typical operating parameters. The fuel cell's health was assessed by examining its cell voltage consistency. A 95.04% accuracy rate was achieved using the random forest algorithm after selecting relevant features. The simulation results were analyzed, and the method had high experimental accuracy and a short computation time compared to SVM. Iskenderoglu et al. [85] used RF for predicting the performance of SOFC units. In the proposed algorithms, each input dataset consisted of ten parameters, including temperature; the concentrations of each component of the anode feeding gas (CO_2, CH_4, N_2, CO, and H_2); current density; the flowrate of equivalent hydrogen; and the type of polarization (forward or backward). The model had one output, i.e., the output voltage of the SOFC fuel cell (or cell working potential), as shown in Figure 26. These algorithms were generated using experimental data with different temperature and hydrogen flow measurements. The authors used 1122 records from the experimental dataset to train the regression algorithm. The model took approximately 0.52 s to predict the cell performance (output voltage), with an average absolute percentage error of 1.97% for RF, as shown in Figure 27.

Lin et al. [86] proposed a random forest algorithm for predicting fuel health based on historical data. Since multiple factors could cause fuel cell problems, feature selection was required in the diagnosis process. Various aspects of hydrogen fuel cell sensor data were explored, and several features were extracted through statistical analysis. The model was also capable of identifying the most important factor for maintaining the fuel cell's health. Chen et al. [87] combined experimental data to design a fuel cell fault detection framework that used random forest to complete the ranking and selection of features to determine the fault type. There were many raw data, and after the initial processing of the data, the features were ranked by random forest, and the final features were selected. Lu et al. [88] studied the system energy optimization of a fuel cell hybrid power robot using comprehensive performance evaluation and random forest prediction methods. With improved power stability and reduced hydrogen consumption, this control method was ideally suited for applications in hybrid welding robots.

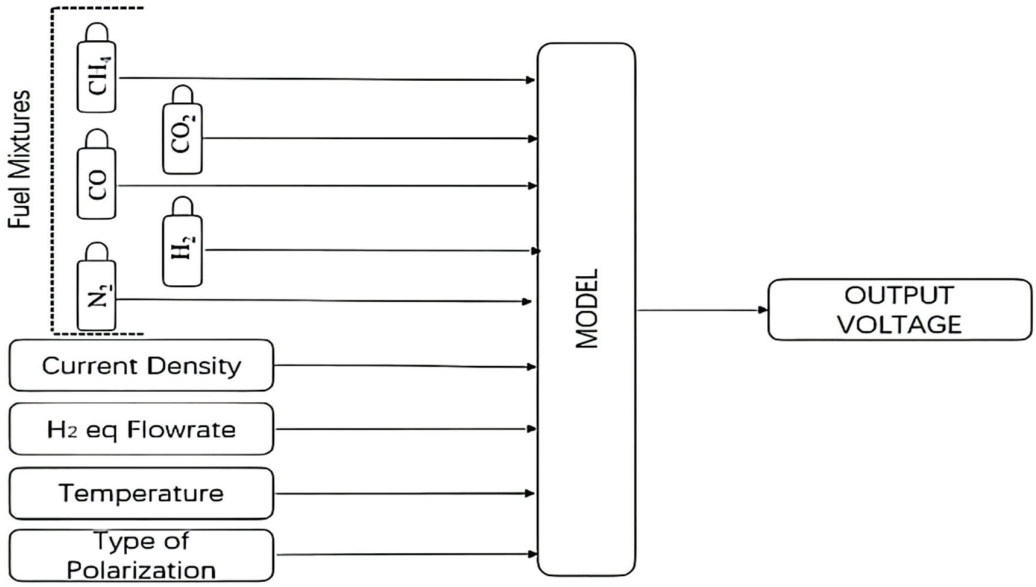


Figure 26. Inputs and output parameters used in proposed algorithms [85].

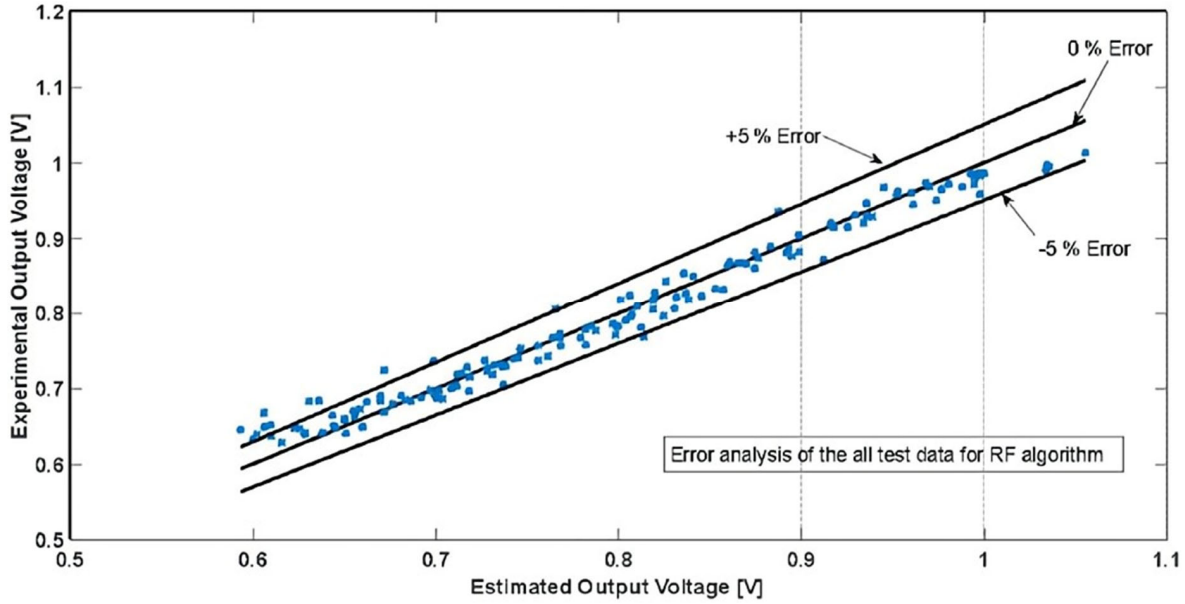


Figure 27. An indicator plot of average absolute percentage error for RF [85].

Guo et al. [89] combined a random forest trained alternative model with a GA to achieve block structure optimization applied to a novel two-block channel. The genetic algorithm was used to optimize the block geometry (length, width, and height) in the flow channel. The genetic algorithm optimization process is shown in Figure 28. The genetic algorithm automatically generated three parameters (block length, width, and height). Then, these three optimization parameters were input into a data-driven surrogate model trained with random forest to calculate the fitness. Finally, the population was selected, crossed and mutated, and iterated until convergence. The results showed that the output values of the surrogate model trained by random forest fit well with the actual values of the physical model. After optimization by the genetic algorithm, the block parameters of 0.6 mm in length, 0.375 mm in width, and 0.75 mm in height were found to be optimal, and the results were validated by the physical model.

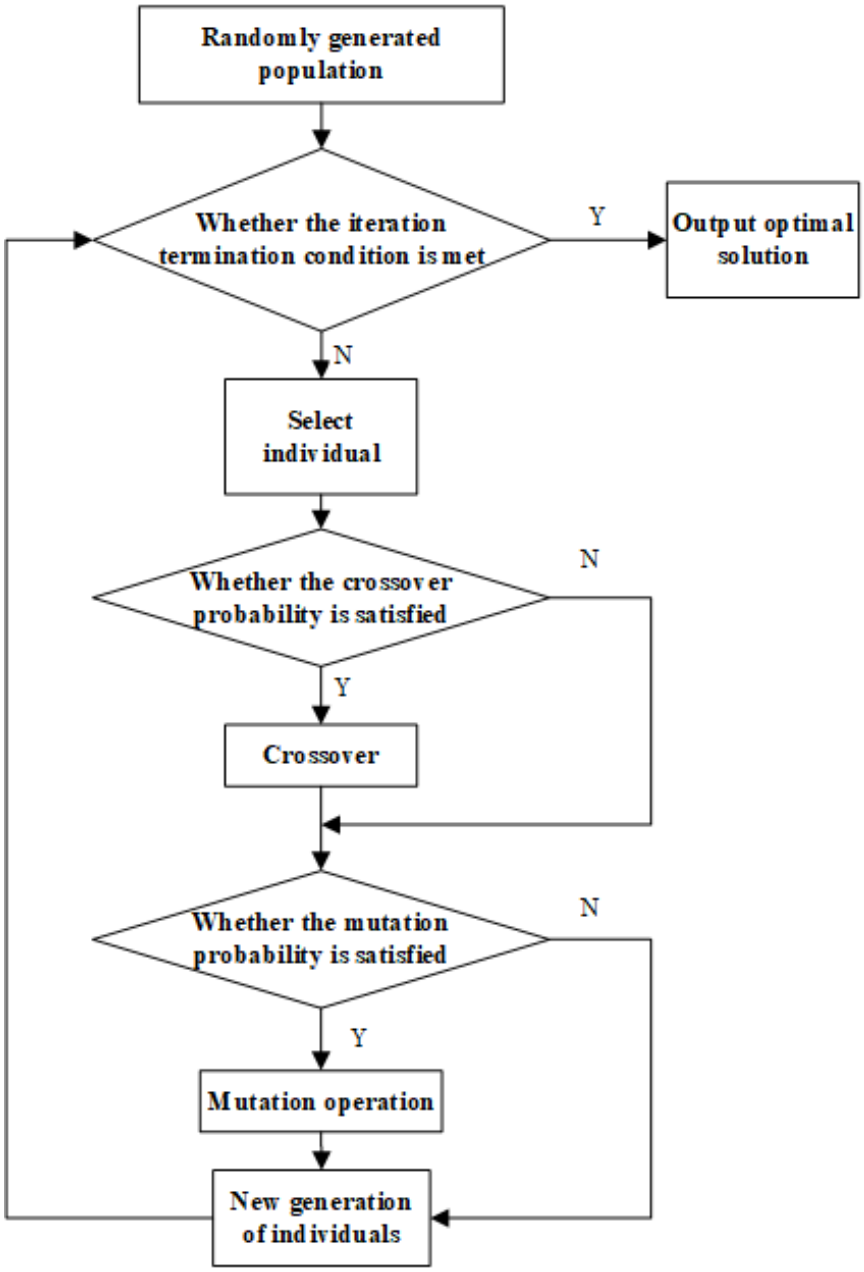


Figure 28. Genetic algorithm flow chart [89].

The dataset was not very large, as show in Figure 18, and k-fold cross-validation was chosen to divide the dataset in order to use the data in the most rational way. The cross-validation schematic is shown in Figure 29. After partitioning the data using a fourfold cross-validation approach and building the alternative models to predict the de-watering time (T) and maximum pressure drop (ΔP) in the channel, the model performance was evaluated separately using the mean square error (MSE).

$$MSE = \sum_{i=1}^{n} \frac{(y_i - A_i)^2}{n} \tag{6}$$

where y_i denotes the actual value of the simulation results from the physical model. The lower the MSE, the higher the accuracy of the model, and the more reliable the prediction results. The method could efficiently optimize the block parameters in the flow channel with a small dataset while satisfying a certain accuracy, providing a promising tool for

achieving better water management. The optimization framework of this study also had promising applications in other areas of fuel cell structure design and the optimization of operating parameters.

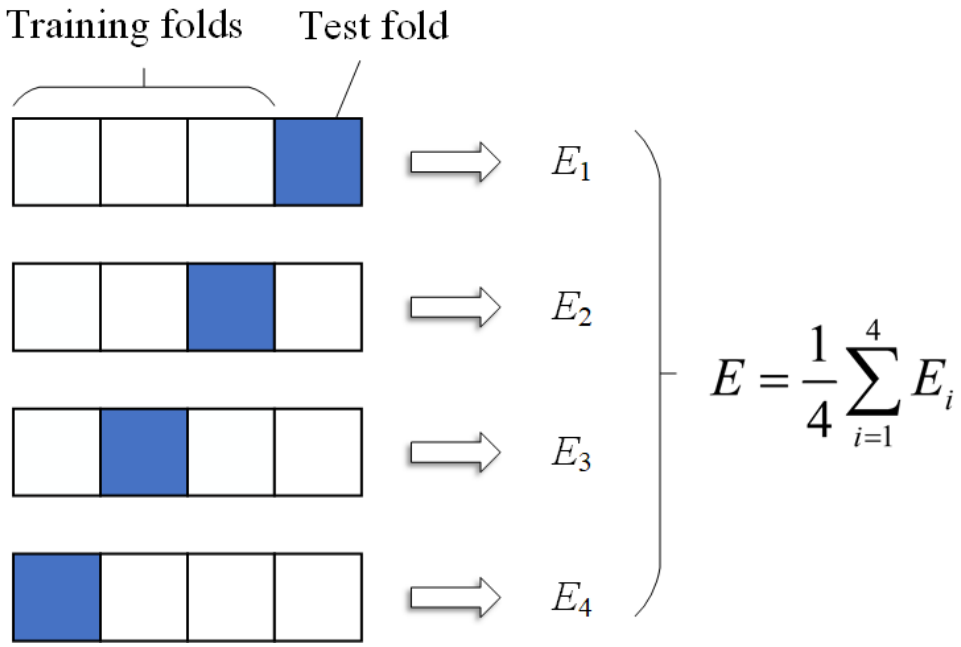


Figure 29. Cross-validation schematic [89].

Figure 30 shows the variation in MSE with the number of decision trees in the water removal time prediction model and in the maximum pressure drop prediction model.

The above three methods have their respective advantages and limitations for research into fuel cells and are applicable to different scenarios. When dealing with large amounts of data and continuous data features, neural networks are the most effective among the three, but the training time is relatively long. For small datasets, RF and SVM are more suitable. Random forest is suitable for non-differentiable models, and one of its advantages is that it can establish the relationship between classification results and input features. SVR is widely used in datasets with a moderate size and obvious relationships. All three methods have classification and prediction functions, with SVM and RF mainly used for classification. However, SVM can also be improved for prediction purposes.

Machine learning, as an emerging technological tool, can play an important role in the design, manufacturing, and operation of fuel cells, but it also faces some challenges: (1) Data acquisition and pre-processing. Fuel cell data are usually high-dimensional, multi-modal, and nonlinear, so effective data acquisition and pre-processing are required, while the quality and accuracy of the data need to be considered. (2) Feature extraction and selection. Feature selection and extraction are key steps in machine learning, but for fuel cell data, it is still a challenge to select the appropriate features. (3) Real-time operation and scalability. The real-time operation and scalability of fuel cells are important challenges for machine learning research, and more efficient and scalable algorithms and models need to be found. In the future, the application of ML in fuel cell research can be explored in the following ways: (1) Research on fuel cell design, such as the selection of catalysts and the optimization of flow channels; (2) the building of more complete fuel cell datasets to provide richer and more accurate data for machine learning algorithms and models; and (3) the development of intelligent fuel cell operation management systems to improve their reliability and safety.

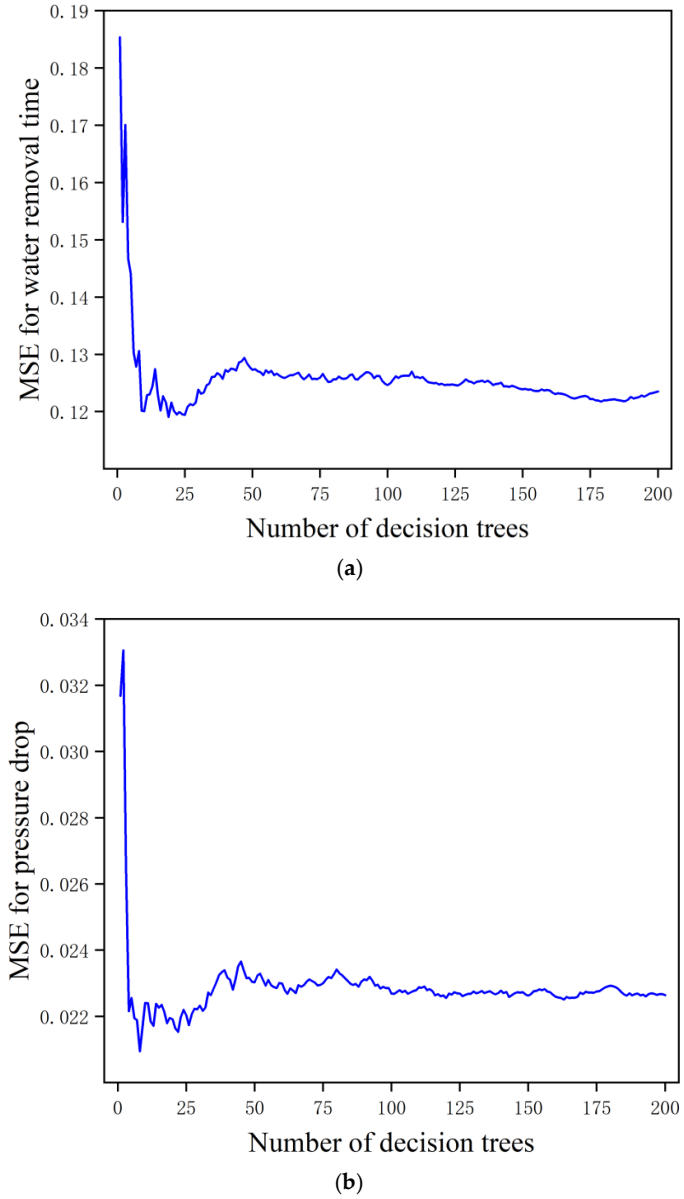


Figure 30. Models with good accuracy: (**a**) water removal time; (**b**) pressure drop [89].

5. Conclusions

Efficient evaluation methods for performance, service life, and fault detection are critical to the design and optimization of fuel cells. The significance and status of machine learning applications in fuel cells were reported; the common machine learning models, including neural network, support vector machine, and random forest models, and intelligent optimization algorithms were described; and the application of common machine learning algorithms in fuel cells was reviewed comprehensively. Machine learning methods can learn from existing data provided by physical models and experiments and then train surrogate models. At present, data-driven surrogate models trained by machine learning methods have shown comparable accuracy to physical models and experimental data of fuel cells and can achieve accurate model prediction results. Data-driven surrogate models can complete most of the calculations within one second, greatly shortening the data procurement time compared to physical CFD models and experimental tests of fuel cells, which may take hundreds of hours. Machine learning methods greatly improve computational efficiency and reduce the workload and experimental or simulation costs. Machine learning algorithms have been successfully used for performance prediction, service life prediction,

and fault diagnosis in fuel cells, achieving considerable accuracy in solving nonlinear problems and presenting good agreement with physical models and experimental data, if an appropriate machine learning model is selected and trained properly. Combinations of machine learning models and intelligent optimization algorithms have shown great advantages, achieving multiple design and operating parameter optimization goals with good accuracy and efficiency.

Funding: This work was financially supported by the National Natural Science Foundation of China (grant no. 51706153).

Data Availability Statement: Data sharing is not applicable to this article as no new data were created or analyzed in this study.

Conflicts of Interest: The authors declare no conflict of interest.

References

1. Giuliano, A.; Errico, M.; Salehi, H.; Avino, P. Environmental Impact Assessment by Green Processes. *Int. J. Environ. Res. Public Health* **2022**, *19*, 15575. [CrossRef] [PubMed]
2. Sallam, E.; Khairy, H.; Elnouby, M.; Fetouh, H. Sustainable electricity production from seawater using Spirulina platensis microbial fuel cell catalyzed by silver nanoparticles-activated carbon composite prepared by a new modified photolysis method. *Biomass Bioenergy* **2021**, *148*, 106038. [CrossRef]
3. Sallam, E.R.; Fetouh, H.A. Comparative Study for the Production of Sustainable Electricity from Marine Sediment Using Recyclable Low-Cost Solid Wastes Aluminum Foil and Graphite Anodes. *ChemistrySelect* **2022**, *7*, 573–591. [CrossRef]
4. Sallam, E.R.; Khairy, H.M.; Elshobary, M.; Fetouh, H.A. *Handbook of Research on Algae as a Sustainable Solution for Food, Energy, and the Environment*; IGI Global: Hershey, PA, USA, 2022; pp. 354–378.
5. Arif, M.; Cheung, S.C.; Andrews, J. Different approaches used for modelling and simulation of Polymer Electrolyte Membrane fuel cells: A Review. *Energy Fuels* **2020**, *34*, 11897–11915. [CrossRef]
6. Sajid, A.; Pervaiz, E.; Ali, H.; Noor, T.; Baig, M.M. A perspective on development of fuel cell materials: Electrodes and electrolyte. *Int. J. Energy Res.* **2022**, *46*, 6953–6988. [CrossRef]
7. Marappan, M.; Palaniswamy, K.; Velumani, T.; Kim, B.C.; Velayutham, R.; Shivakumar, P.; Sundaram, S. Performance Studies of Proton Exchange Membrane Fuel Cells with Different Flow Field Designs—Review. *Chem. Rec.* **2021**, *21*, 663–714. [CrossRef]
8. Wu, C.; Zhang, W.; Han, X.; Zhang, Y.; Ma, G. A systematic review for structure optimization and clamping load design of large proton exchange membrane fuel cell stack. *J. Power Sources* **2020**, *476*, 228724. [CrossRef]
9. Daud, W.; Rosli, R.; Majlan, E.; Hamid, S.; Mohamed, R.; Husaini, T. PEM fuel cell system control: A review. *Renew. Energy* **2017**, *113*, 620–638. [CrossRef]
10. Mohammed, A.S.; Atnaw, S.M.; Salau, A.O.; Eneh, J.N. Review of optimal sizing and power management strategies for fuel cell/battery/super capacitor hybrid electric vehicles. *Energy Rep.* **2023**, *9*, 2213–2228. [CrossRef]
11. Kloess, J.P.; Wang, X.; Liu, J.; Shi, Z.; Guessous, L. Investigation of bio-inspired flow channel designs for bipolar plates in proton exchange membrane fuel cells. *J. Power Sources* **2009**, *188*, 132–140. [CrossRef]
12. Huang, H.; Lei, H.; Liu, M.; Wang, T.; Li, C.; Guo, X.; Chen, Y.; Pan, M. Effect of superior mesenteric artery branch structure-based flow field on PEMFC performance. *Energy Convers. Manag.* **2020**, *226*, 113546. [CrossRef]
13. Xing, L.; Shi, W.; Su, H.; Xu, Q.; Das, P.K.; Mao, B.; Scott, K. Membrane electrode assemblies for PEM fuel cells: A review of functional graded design and optimization. *Energy* **2019**, *177*, 445–464. [CrossRef]
14. Li, X.; Wang, Y.; Yang, D.; Chen, Z. Adaptive energy management strategy for fuel cell/battery hybrid vehicles using Pontryagin's Minimal Principle. *J. Power Sources* **2019**, *440*, 227105. [CrossRef]
15. Wang, B.; Xie, B.; Xuan, J.; Jiao, K. AI-based optimization of PEM fuel cell catalyst layers for maximum power density via data-driven surrogate modeling. *Energy Convers. Manag.* **2020**, *205*, 112460. [CrossRef]
16. Kong, X.; Khambadkone, A.M. Modeling of a PEM fuel-cell stack for dynamic and steady-state operation using ANN-based submodels. *IEEE Trans. Ind. Electron.* **2009**, *56*, 4903–4914. [CrossRef]
17. Huo, H.; Ji, Y.; Kuang, X.; Liu, Y.; Wu, Y. Dynamic modeling of SOFC based on support vector regression machine and improved particle swarm optimization. In Proceedings of the 11th World Congress on Intelligent Control and Automation, Shenyang, China, 29 June–4 July 2014; pp. 1853–1858.
18. Kheirandish, A.; Shafiabady, N.; Dahari, M.; Kazemi, M.S.; Isa, D. Modeling of commercial proton exchange membrane fuel cell using support vector machine. *Int. J. Hydrogen Energy* **2016**, *41*, 11351–11358. [CrossRef]
19. Ding, R.; Yin, W.; Cheng, G. Effectively increasing Pt utilization efficiency of the membrane electrode assembly in proton exchange membrane fuel cells through multiparameter optimization guided by machine learning. *ACS Appl. Mater. Interfaces* **2022**, *14*, 8010–8024. [CrossRef]
20. Chen, H.; Shan, W.; Liao, H.; He, Y.; Zhang, T.; Pei, P.; Deng, C.; Chen, J. Online voltage consistency prediction of proton exchange membrane fuel cells using a machine learning method. *Int. J. Hydrogen Energy* **2021**, *46*, 34399–34412. [CrossRef]

21. Raeesi, M.; Changizian, S.; Ahmadi, P.; Khoshnevisan, A. Performance analysis of a degraded PEM fuel cell stack for hydrogen passenger vehicles based on machine learning algorithms in real driving conditions. *Energy Convers. Manag.* **2021**, *248*, 114793. [CrossRef]
22. Li, Z.; Giurgea, S.; Outbib, R.; Hissel, D. Fault diagnosis and novel fault type detection for PEMFC system based on spherical-shaped multiple-class support vector machine. In Proceedings of the 2014 IEEE/ASME International Conference on Advanced Intelligent Mechatronics, Besacon, France, 8–11 July 2014; pp. 1628–1633.
23. Zheng, Y.; Wu, X.-L.; Zhao, D.; Xu, Y.-W.; Wang, B.; Zu, Y.; Li, D.; Jiang, J.; Jiang, C.; Fu, X.; et al. Data-driven fault diagnosis method for the safe and stable operation of solid oxide fuel cells system. *J. Power Sources* **2021**, *490*, 229561. [CrossRef]
24. Chen, K.; Laghrouche, S.; Djerdir, A. Remaining useful life prediction for fuel Cell based on support vector regression and grey wolf optimizer algorithm. *IEEE Trans. Energy Convers.* **2022**, *37*, 778–787. [CrossRef]
25. Castro, J.L.; Mantas, C.J.; Benítez, J.M. Neural networks with a continuous squashing function in the output are universal approximators. *Neural Netw.* **2000**, *13*, 561–563. [CrossRef]
26. Wang, L.; Zeng, Y.; Tao, C. Back propagation neural network with adaptive differential evolution algorithm for time series forecasting. *Expert Syst. Appl.* **2015**, *42*, 855–863. [CrossRef]
27. Al-Othman, A.; Tawalbeh, M.; Martis, R.; Dhou, S.; Orhan, M.; Qasim, M.; Olabi, A.G. Artificial intelligence and numerical models in hybrid renewable energy systems with fuel cells: Advances and prospects. *Energy Convers. Manag.* **2022**, *253*, 115154. [CrossRef]
28. Kim, H.-C.; Pang, S.; Je, H.-M.; Kim, D.; Bang, S.Y. Constructing support vector machine ensemble. *Pattern Recognit.* **2003**, *36*, 2757–2767. [CrossRef]
29. Zhang, H.; Wang, Z.; Liu, D. A comprehensive review of stability analysis of continuous-time recurrent neural networks. *IEEE Trans. Neural Netw. Learn. Syst.* **2014**, *25*, 1229–1262. [CrossRef]
30. Tian, Y. Artificial intelligence image recognition method based on convolutional neural network algorithm. *IEEE Access* **2020**, *8*, 125731–125744. [CrossRef]
31. Zhang, X.; Jiang, R.; Wang, T.; Wang, J. Recursive neural network for video deblurring. *IEEE Trans. Circuits Syst. Video Technol.* **2021**, *31*, 3025–3036. [CrossRef]
32. Pourrahmani, H.; Moghimi, M.; Siavashi, M. Thermal management in PEMFCs: The respective effects of porous media in the gas flow channel. *Int. J. Hydrogen Energy* **2019**, *44*, 3121–3137. [CrossRef]
33. Ahadian, S.; Khajeh-Hosseini-Dalasm, N.; Fushinobu, K.; Okazaki, K.; Kawazoe, Y. An effective computational approach to the parametric study of the cathode catalyst layer of PEM fuel cells. *Mater. Trans.* **2011**, *52*, 1954–1959. [CrossRef]
34. Hwang, H.; Choi, S.M.; Oh, J.; Bae, S.-M.; Lee, J.-H.; Ahn, J.-P.; Lee, J.-O.; An, K.-S.; Yoon, Y.; Hwang, J.-H. Integrated application of semantic segmentation-assisted deep learning to quantitative multi-phased microstructural analysis in composite materials: Case study of cathode composite materials of solid oxide fuel cells. *J. Power Sources* **2020**, *471*, 228458. [CrossRef]
35. Liu, X.; Yan, Z.; Zhong, Z. Predicting elastic modulus of porous La0.6Sr0.4Co0.2Fe0.8O3-δ cathodes from microstructures via FEM and deep learning. *Int. J. Hydrogen Energy* **2021**, *46*, 22079–22091. [CrossRef]
36. Khajeh-Hosseini-Dalasm, N.; Ahadian, S.; Fushinobu, K.; Okazaki, K.; Kawazoe, Y. Prediction and analysis of the cathode catalyst layer performance of proton exchange membrane fuel cells using artificial neural network and statistical methods. *J. Power Sources* **2011**, *196*, 3750–3756. [CrossRef]
37. Seyhan, M.; Akansu, Y.E.; Murat, M.; Korkmaz, Y.; Akansu, S.O. Performance prediction of PEM fuel cell with wavy serpentine flow channel by using artificial neural network. *Int. J. Hydrogen Energy* **2017**, *42*, 25619–25629. [CrossRef]
38. Lopes, F.D.C.; Watanabe, E.H.; Rolim, L.G.B. A control-oriented model of a PEM fuel cell stack based on NARX and NOE neural networks. *IEEE Trans. Ind. Electron.* **2015**, *62*, 5155–5163. [CrossRef]
39. He, K.; Zhang, C.; He, Q.; Wu, Q.; Jackson, L.; Mao, L. Effectiveness of PEMFC historical state and operating mode in PEMFC prognosis. *Int. J. Hydrogen Energy* **2020**, *45*, 32355–32366. [CrossRef]
40. Lee, W.; Park, G.; Yang, T.; Yoon, Y.; Kim, C. Empirical modeling of polymer electrolyte membrane fuel cell performance using artificial neural networks. *Int. J. Hydrogen Energy* **2004**, *29*, 961–966. [CrossRef]
41. Saengrung, A.; Abtahi, A.; Zilouchian, A. Neural network model for a commercial PEM fuel cell system. *J. Power Sources* **2007**, *172*, 749–759. [CrossRef]
42. Napoli, G.; Ferraro, M.; Sergi, F.; Brunaccini, G.; Antonucci, V. Data driven models for a PEM fuel cell stack performance prediction. *Int. J. Hydrogen Energy* **2013**, *38*, 11628–11638. [CrossRef]
43. Marra, D.; Sorrentino, M.; Pianese, C.; Iwanschitz, B. A neural network estimator of Solid Oxide Fuel Cell performance for on-field diagnostics and prognostics applications. *J. Power Sources* **2013**, *241*, 320–329. [CrossRef]
44. Jian, Q.; Wu, H. The simulation study on dynamic characteristics of PEMFC based on BP neural network optimized by genetic algorithm. *J. Jiangxi Norm. Univ.* **2015**, *3*, 221–229.
45. Dang, H.; Ma, R.; Zhou, J.; Huangfu, Y. Falut diagnosis of proton exchange membrane fuel cells based on CNN. *Power Electron.* **2020**, *54*, 52–55.
46. Bicer, Y.; Dincer, I.; Aydin, M. Maximizing performance of fuel cell using artificial neural network approach for smart grid applications. *Energy* **2016**, *116*, 1205–1217. [CrossRef]
47. Wang, L.; Zhang, H.; Tang, M. Stability and dynamics prediction of PEMFC based on BP neural network. *Power Technol.* **2017**, *41*, 871–873.

48. Yan, F.; Li, W.; Yang, W.; He, Y. Prediction of fuel cell performance based on Bagging neural network ensemble model. *Sci. Sin. Technol.* **2019**, *49*, 391–401. [CrossRef]
49. Barzegari, M.M.; Rahgoshay, S.M.; Mohammadpour, L.; Toghraie, D. Performance prediction and analysis of a dead-end PEMFC stack using data-driven dynamic model. *Energy* **2019**, *188*, 116049. [CrossRef]
50. Tsompanas, M.-A.; You, J.; Wallis, L.; Greenman, J.; Ieropoulos, I. Artificial neural network simulating microbial fuel cells with different membrane materials and electrode configurations. *J. Power Sources* **2019**, *436*, 226832. [CrossRef]
51. Laribi, S.; Mammar, K.; Hamouda, M.; Sahli, Y. Impedance model for diagnosis of water management in fuel cells using artificial neural networks methodology. *Int. J. Hydrogen Energy* **2016**, *41*, 17093–17101. [CrossRef]
52. Arama, F.Z.; Mammar, K.; Laribi, S.; Necaibia, A.; Ghaitaoui, T. Implementation of sensor based on neural networks technique to predict the PEM fuel cell hydration state. *J. Energy Storage* **2020**, *27*, 101051. [CrossRef]
53. Guo, C.; Lu, J.; Tian, Z.; Guo, W.; Darvishan, A. Optimization of critical parameters of PEM fuel cell using TLBO-DE based on Elman neural network. *Energy Convers. Manag.* **2019**, *183*, 149–158. [CrossRef]
54. Morando, S.; Jemei, S.; Hissel, D.; Gouriveau, R.; Zerhouni, N. Proton exchange membrane fuel cell ageing forecasting algorithm based on Echo State Network. *Int. J. Hydrogen Energy* **2016**, *42*, 1472–1480. [CrossRef]
55. Morando, S.; Jemei, S.; Hissel, D.; Gouriveau, R.; Zerhouni, N. ANOVA method applied to proton exchange membrane fuel cell ageing forecasting using an echo state network. *Math. Comput. Simul.* **2017**, *131*, 283–294. [CrossRef]
56. Heidary, H.; Kermani, M.J.; Dabir, B. Influences of bipolar plate channel blockages on PEM fuel cell performances. *Energy Convers. Manag.* **2016**, *124*, 51–60. [CrossRef]
57. Wang, Y. Simulation Analysis of Water Management in Proton Exchange Membrane Fuel Cells. Master's Thesis, North China University of Water Resources and Hydropower, Zhengzhou, China, 2020.
58. Fan, L.; Niu, Z.; Zhang, G.; Jiao, K. Optimization design of the cathode flow channel for proton exchange membrane fuel cells. *Energy Convers. Manag.* **2018**, *171*, 1813–1821. [CrossRef]
59. Perng, S.; Wu, H. A three-dimensional numerical investigation of trapezoid baffles effect on non-isothermal reactant transport and cell net power in a PEMFC. *Appl. Energy* **2015**, *143*, 81–95. [CrossRef]
60. Pourrahmani, H.; Siavashi, M.; Moghimi, M. Design optimization and thermal management of the PEMFC using artificial neural networks. *Energy* **2019**, *182*, 443–459. [CrossRef]
61. Pourrahmani, H.; Moghimi, M.; Siavashi, M.; Shirbani, M. Sensitivity analysis and performance evaluation of the PEMFC using wave-like porous ribs. *Appl. Therm. Eng.* **2019**, *150*, 433–444. [CrossRef]
62. Li, W.; Yan, F.; Deng, Y. Sensitivity analysis and optimization of block height in PEMFC cathode runners. *J. Eng. Thermophys.* **2020**, *41*, 697–703.
63. Guo, Q.; Zheng, J.; Qin, Y. Optimization of block structure parameters of PEMFC novel block channels using artificial neural network. *Int. J. Hydrogen Energy* **2022**, *90*, 38386–38394. [CrossRef]
64. Guo, Q.; Qin, Y. Numerical investigation of water droplet removal characteristics in novel block channels of PEMFC using dynamic wettability model. *Int. J. Hydrogen Energy* **2021**, *46*, 36890–36902. [CrossRef]
65. Yang, Z.; Wang, B.; Sheng, X.; Wang, Y.; Ren, Q.; He, S.; Xuan, J.; Jiao, K. An artificial intelligence solution for predicting short-term degradation behaviors of proton exchange membrane fuel cell. *Appl. Sci.* **2021**, *11*, 6348. [CrossRef]
66. Zuo, J.; Lv, H.; Zhou, D.; Xue, Q.; Jin, L.; Zhou, W.; Yang, D.; Zhang, C. Deep learning based prognostic framework towards proton exchange membrane fuel cell for automotive application. *Appl. Energy* **2021**, *281*, 115937. [CrossRef]
67. Ma, R.; Yang, T.; Breaz, E.; Li, Z.; Briois, P.; Gao, F. Data-driven proton exchange membrane fuel cell degradation predication through deep learning method. *Appl. Energy* **2018**, *231*, 102–115. [CrossRef]
68. Wang, F.-K.; Cheng, X.-B.; Hsiao, K.-C. Stacked long short-term memory model for proton exchange membrane fuel cell systems degradation. *J. Power Sources* **2020**, *448*, 227591. [CrossRef]
69. Jeme, S.; Hissel, D.; Péra, M.C.; Kauffmann, J.M. On-board fuel cell power supply modeling on the basis of neural network methodology. *J. Power Sources* **2003**, *124*, 479–486. [CrossRef]
70. Xu, H.; Ma, J.; Tan, P.; Chen, B.; Wu, Z.; Zhang, Y.; Wang, H.; Xuan, J.; Ni, M. Towards online optimization of solid oxide fuel cell performance: Combining deep learning with multi-physics simulation. *Energy AI* **2020**, *1*, 100003. [CrossRef]
71. Legala, A.; Zhao, J.; Li, X. Machine learning modeling for proton exchange membrane fuel cell performance. *Energy AI* **2022**, *10*, 100183. [CrossRef]
72. Chauhan, V.; Mortazavi, M.; Benner, J.Z.; Santamaria, A.D. Two-phase flow characterization in PEM fuel cells using machine learning. *Energy Rep.* **2020**, *6*, 2713–2719. [CrossRef]
73. Han, I.S.; Chung, C.B. Performance prediction and analysis of a PEM fuel cell operating on pure oxygen sing data-driven models: A comparison of artificial neural network and support vector machine. *Int. J. Hydrogen Energy* **2016**, *41*, 10202–10211. [CrossRef]
74. Zou, W.; Froning, D.; Shi, Y.; Lehnert, W. Working zone for a least-squares support vector machine for modeling polymer electrolyte fuel cell voltage. *Appl. Energy* **2021**, *283*, 116191. [CrossRef]
75. Li, X.; Cao, G.-Y.; Zhu, X.-J. Modeling and control of PEMFC based on least squares support vector machines. *Energy Convers. Manag.* **2006**, *47*, 1032–1050. [CrossRef]
76. Han, I.-S.; Chung, C.-B. A hybrid model combining a support vector machine with an empirical equation for predicting polarization curves of PEM fuel cells. *Int. J. Hydrogen Energy* **2017**, *42*, 7023–7028. [CrossRef]

77. Peng, X.; Wu, W.; Zhang, Y.; Yang, W. Determination of operating parameters for PEM fuel cell using support vector machines approach. *J. Energy Storage* **2017**, *13*, 409–417. [CrossRef]
78. Huo, W.; Li, W.; Sun, C.; Ren, Q.; Gong, G. Research on fuel cell fault diagnosis based on genetic algorithm optimization of support vector machine. *Energies* **2022**, *15*, 2294. [CrossRef]
79. Zou, Q.; Tian, Y.; Li, H.; Qin, S. Hydrogen leakage detection method for fuel cell engine based on support vector machine. *J. Beijing Jiaotong Univ.* **2020**, *44*, 84–90.
80. Li, Z.; Outbib, R.; Giurgea, S.; Hissel, D.; Jemei, S.; Giraud, A.; Rosini, S. Online implementation of SVM based fault diagnosis strategy for PEMFC systems. *Appl. Energy* **2016**, *164*, 284–293. [CrossRef]
81. Huo, H.; Huo, H.; Yang, C. Support vector machine (SVM) discriminative modeling of SOFC. *J. Syst. Simul.* **2010**, *22*, 1557–1560.
82. Elcicek, H.; Özdemir, O.K. Prediction of electrocatalyst performance of Pt/C using response surface optimization algorithm-based machine learning approaches. *Int. J. Energy Res.* **2022**, *46*, 21353–21372. [CrossRef]
83. Huo, W.; Li, W.; Zhang, Z.; Sun, C.; Zhou, F.; Gong, G. Performance prediction of proton-exchange membrane fuel cell based on convolutional neural network and random forest feature selection. *Energy Convers. Manag.* **2021**, *243*, 114367. [CrossRef]
84. Pang, R.; Zhang, C.; Dai, H.; Bai, Y.; Hao, D.; Chen, J.; Zhang, B. Intelligent health states recognition of fuel cell by cell voltage consistency under typical operating parameters. *Appl. Energy* **2022**, *305*, 117735. [CrossRef]
85. Iskenderoğlu, F.C.; Baltacioğlu, M.K.; Demir, M.H.; Baldinelli, A.; Barelli, L.; Bidini, G. Comparison of support vector regression and random forest algorithms for estimating the SOFC output voltage by considering hydrogen flow rates. *Int. J. Hydrogen Energy* **2020**, *45*, 35023–35038. [CrossRef]
86. Lin, R.-H.; Pei, Z.-X.; Ye, Z.-Z.; Guo, C.-C.; Wu, B.-D. Hydrogen fuel cell diagnostics using random forest and enhanced feature selection. *Int. J. Hydrogen Energy* **2020**, *45*, 10523–10535. [CrossRef]
87. Chen, M.; Fu, X.; Deng, Z. Data-driven fault detection for SOFC system based on random forest and SVM. In Proceedings of the Chinese Automation Congress (CAC), Hangzhou, China, 22–24 November 2019; pp. 2829–2834.
88. Lü, X.; Deng, R.; Chen, C.; Wu, Y.; Meng, R.; Long, L. Performance optimization of fuel cell hybrid power robot based on power demand prediction and model evaluation. *Appl. Energy* **2022**, *316*, 119087. [CrossRef]
89. Zheng, J.; Qin, Y.; Guo, Q.; Dong, Z.; Zhu, C.; Wang, Y. Block structure optimization in PEMFC flow channels using a data-driven surrogate model based on random forest. *Int. J. Green Energy* **2022**, *90*, 337–346. [CrossRef]

Disclaimer/Publisher's Note: The statements, opinions and data contained in all publications are solely those of the individual author(s) and contributor(s) and not of MDPI and/or the editor(s). MDPI and/or the editor(s) disclaim responsibility for any injury to people or property resulting from any ideas, methods, instructions or products referred to in the content.